medRxiv preprint doi: https://doi.org/10.1101/2024.01.03.24300768; this version posted January 5, 2024. The copyright holder for this preprint (which was not certified by peer review) is the author/funder, who has granted medRxiv a license to display the preprint in perpetuity. It is made available under a CC-BY-NC-ND 4.0 International license .

Multi-ancestry transcriptome-wide association studies of cognitive function, white matter hyperintensity, and Alzheimer's disease

Chaar, Dima L.[1], Li, Zheng[2], Shang, Lulu[3], Ratliff, Scott M.[1], Mosley, Thomas H.[1,4], Kardia, Sharon L.R. [1], Zhao, Wei[1,5], Zhou, X.[2], Smith, J.A.[1,5]

[1] Department of Epidemiology, School of Public Health, University of Michigan, Ann Arbor, Michigan, United States of America
[2] Department of Biostatistics, School of Public Health, University of Michigan, Ann Arbor, Michigan, United States of America
[3] Department of Biostatistics, University of Texas MD Anderson Cancer Center, Houston, Texas, United States of America
[4] Memory Impairment and Neurodegenerative Dementia (MIND) Center, University of Mississippi Medical Center, Jackson, Mississippi
[5] Survey Research Center, Institute for Social Research, University of Michigan, Ann Arbor, Michigan, United States of America

*Corresponding author:

Jennifer A. Smith, PhD, MPH
Department of Epidemiology
University of Michigan
1415 Washington Heights, #2631
Ann Arbor, MI 48109-2029
Phone: 734-615-9455
Fax: 734-764-3192
Email: smjenn@umich.edu
ORCID: 0000-0002- 3575-5468

medRxiv preprint doi: https://doi.org/10.1101/2024.01.03.24300768; this version posted January 5, 2024. The copyright holder for this preprint (which was not certified by peer review) is the author/funder, who has granted medRxiv a license to display the preprint in perpetuity. It is made available under a CC-BY-NC-ND 4.0 International license .

Author Summary

Transcriptome-wide association studies (TWAS) can be used to understand the mechanisms of gene expression that underly disease etiology. However, to date, TWAS methods have mostly been used in a single ancestry group, especially European ancestry (EA), and few TWAS have focused on cognitive function or structural brain measures. We used a newly developed TWAS method called the Multi-ancEstry TRanscriptOme-wide analysis (METRO) to incorproate gene expression data from 801 EA and 1,032 African ancestry (AA) adults to identify genes associated with general cognitive function, structural brain changes called white matter hyperintensities (WMH) that predispose people to vascular dementia, and another form of dementia called Alzheimer's disease (AD). We found that reduced gene expression of *ICA1L* was associated with more WMH and with AD, indicating its potential contribution to overlapping AD and vascular dementia neuropathologies. To our knowledge, our study is the first TWAS of cognitive function and neurocognitive disorders using multiple ancestries. This work may expand the benefits of TWAS studies beyond a single ancestry group and help to identify gene targets for pharmaceutical or preventative treatment for dementia.

medRxiv preprint doi: https://doi.org/10.1101/2024.01.03.24300768; this version posted January 5, 2024. The copyright holder for this preprint (which was not certified by peer review) is the author/funder, who has granted medRxiv a license to display the preprint in perpetuity. It is made available under a CC-BY-NC-ND 4.0 International license .

Abstract

Genetic variants increase the risk of neurocognitive disorders in later life including Vascular Dementia (VaD) and Alzheimer's disease (AD), but the precise relationships between genetic risk factors and underlying disease etiology are not well understood. Transcriptome-wide association studies (TWAS) can be leveraged to better characterize the genes and biological pathways underlying genetic influences on disease. To date, almost all existing TWAS have been conducted using expression studies from individuals of a single genetic ancestry, primarily European. Using the joint likelihood-based inference framework in Multi-ancEstry TRanscriptOme-wide analysis (METRO), we leveraged gene expression data from European (EA) and African ancestries (AA) to identify genes associated with general cognitive function, white matter hyperintensity (WMH), and AD. Regions were fine-mapped using Fine-mapping Of CaUsal gene Sets (FOCUS). We identified 266, 23, 69, and 2 genes associated with general cognitive function, WMH, AD (using EA GWAS summary statistics), and AD (using AA GWAS), respectively (Bonferroni-corrected alpha=$P<2.9x10^{-6}$), some of which were previously identified. Enrichment analysis showed that many of the identified genes were in pathways related to innate immunity, vascular dysfunction, and neuroinflammation. Further, downregulation of *ICA1L* was associated with higher WMH and with AD, indicating its potential contribution to overlapping AD and VaD neuropathology. To our knowledge, our study is the first TWAS of cognitive function and neurocognitive disorders that used expression mapping studies in multiple ancestries. This work may expand the benefits of TWAS studies beyond a single ancestry group and help to identify gene targets for pharmaceutical or preventative treatment for dementia.

medRxiv preprint doi: https://doi.org/10.1101/2024.01.03.24300768; this version posted January 5, 2024. The copyright holder for this preprint (which was not certified by peer review) is the author/funder, who has granted medRxiv a license to display the preprint in perpetuity. It is made available under a CC-BY-NC-ND 4.0 International license .

90

medRxiv preprint doi: https://doi.org/10.1101/2024.01.03.24300768; this version posted January 5, 2024. The copyright holder for this preprint (which was not certified by peer review) is the author/funder, who has granted medRxiv a license to display the preprint in perpetuity. It is made available under a CC-BY-NC-ND 4.0 International license .

Introduction

Adult-onset dementia is comprised of a group of aging-related neurocognitive disorders caused by the gradual degeneration of neurons and the loss of brain function. These changes lead to a decline in cognitive abilities and impairment of daily activities and independent function. In the United States, Alzheimer's disease (AD), the most common cause of dementia, affects 6.8 million adults age 65 and older (1). The second most common form of dementia is vascular dementia (VaD), which often co-occurs with AD and is underdiagnosed (1,2). VaD is often difficult to distinguish from AD because these diseases share cognitive symptoms including noticeable impairment in episodic and semantic memory. While AD and VaD often co-occur, each form of dementia has differing pathophysiology that may precede the illness decades prior.

AD is characterized by aggregation of amyloid-beta protein and neurofibrillary tangles in brain tissue (3,4), while VaD may be caused by reduced blood flow to the brain as a result of small vessel disease (SVD) or stroke and is commonly seen in people with hypertension (5). AD is diagnosed based on a battery of memory tests, brain-imaging tests for degeneration of brain cells and laboratory tests to assess the presence of amyloid and tau proteins in cerebrospinal fluid (6). SVD is primarily detected on magnetic resonance imaging (MRI) as white matter hyperintensities (WMH). It has been hypothesized that vascular and neurodegenerative changes in the brain may interact in ways that increase the likelihood of cognitive impairment. A further challenge in the field is distinguishing between individuals who are aging normally from those with dementia pathology.

A greater understanding of the pathological processes that influence cognitive function in older adults is critical for early intervention during the long preclinical or prodromal phase prior to dementia onset, especially in vulnerable populations (7,8). For example, individuals of African

medRxiv preprint doi: https://doi.org/10.1101/2024.01.03.24300768; this version posted January 5, 2024. The copyright holder for this preprint (which was not certified by peer review) is the author/funder, who has granted medRxiv a license to display the preprint in perpetuity. It is made available under a CC-BY-NC-ND 4.0 International license .

ancestry (AA) have a greater burden of and risk for developing dementia compared to Non-Hispanic Whites (9–12). Differences in gene expression, which are influenced by both genetic and non-genetic factors, likely play a role in shaping racial/ethnic health disparities in neurological outcomes. However, the underlying molecular and environmental mechanisms that influence gene expression are not fully understood, especially in populations with non-European ancestries. Given the multifactorial and complex nature of dementia, multi-omic data integration across ancestry groups may lend insight into these disparities, allowing the identification of targets for intervention and treatment in populations that are most at risk (13).

Genome-wide association studies (GWAS) have identified genetic variants associated with cognitive function and dementia; however, most GWAS variants are located in non-coding regions so their functional consequences are difficult to characterize (14). Transcriptome-wide association studies (TWAS) utilize gene expression and genetic data to increase power for identifying gene-trait associations and characterizing transcriptomic mechanisms underlying complex diseases. To date, however, few TWAS have been conducted on cognitive or structural brain measures. Further, previous TWAS have primarily been conducted in populations of European ancestry (EA), but these results cannot always be generalized to other genetic ancestries due to differences in allele frequencies, patterns of linkage disequilibrium (LD), and relationships between SNPs and gene expression between populations (15–18). To better identify gene-trait associations in non-EA ancestries, it is necessary to incorporate results from recent expression quantitative trait locus (eQTL) mapping studies, which identify genetic variants that explain variations in gene expression levels, conducted in different ancestry groups.(19)

Multi-ancEstry TRanscriptOme-wide analysis (METRO)(20) is a TWAS method that uses a joint likelihood-based inference framework to borrow complementary information across

medRxiv preprint doi: https://doi.org/10.1101/2024.01.03.24300768; this version posted January 5, 2024. The copyright holder for this preprint (which was not certified by peer review) is the author/funder, who has granted medRxiv a license to display the preprint in perpetuity. It is made available under a CC-BY-NC-ND 4.0 International license .

multiple ancestries to increase TWAS power. In this study, we used genotype and gene expression data from 1,032 AA and 801 EA from the Genetic Epidemiology Network of Arteriopathy (GENOA) and summary statistics from published GWAS (21–24) to identify genes associated with general cognitive function, white matter hyperintensity, and AD. We then examined the contribution of different ancestry-dependent transcriptomic profiles on the gene-trait associations. Greater knowledge of the underlying molecular mechanisms of dementia that are generalizable to both EA and AA is a critical step in evaluating potential causal variants and genes that could be targeted for pharmaceutical development.

2. Materials and Methods

2.1. Sample

The Genetic Epidemiology Network of Arteriopathy (GENOA)

The GENOA study is a community-based longitudinal study aimed at examining the genetic effects of hypertension and related target organ damage (25). EA and AA hypertensive sibships were recruited if at least 2 siblings were clinically diagnosed with hypertension before age 60. All other siblings were invited to participate, regardless of their hypertension status. Exclusion criteria included secondary hypertension, alcoholism or drug abuse, pregnancy, insulin-dependent diabetes mellitus, active malignancy, or serum creatinine levels >2.5mg/dL. In Phase I (1996-2001), 1,854 AA participants (Jackson, MS) and 1,583 EA participants (Rochester, MN) were recruited (25). In Phase II (2000-2004), 1,482 AA and 1,239 EA participants were successfully followed up, and their potential target organ damage from hypertension was measured. Demographics, medical history, clinical characteristics, information on medication use, and blood samples were collected in each phase. After data cleaning and

medRxiv preprint doi: https://doi.org/10.1101/2024.01.03.24300768; this version posted January 5, 2024. The copyright holder for this preprint (which was not certified by peer review) is the author/funder, who has granted medRxiv a license to display the preprint in perpetuity. It is made available under a CC-BY-NC-ND 4.0 International license .

quality control, a total of 1,032 AA and 801 EA with genotype and gene expression data were available for analysis. Written informed consent was obtained from all participants, and approval was granted by participating institutional review boards (University of Michigan, University of Mississippi Medical Center, and Mayo Clinic).

2.2. Measures

2.2.1. Genetic Data

AA and EA blood samples were genotyped using the Affymetrix® Genome-Wide Human SNP Array 6.0 or the Illumina 1M Duo. We followed the procedures outlined by Shang et al.(18) for data processing. For each platform, samples and SNPs with a call rate <95%, samples with mismatched sex, and duplicate samples were excluded. After removing outliers identified from genetic principal component analysis, there were 1,599 AA and 1,464 EA with available genotype data. Imputation was performed using the Segmented HAPlotype Estimation & Imputation Tool (SHAPEIT) v.2.r(26) and IMPUTE v.2(27) using the 1000 Genomes project phase I integrated variant set release (v.3) in NCBI build 37 (hg19) coordinates (released in March 2012). Imputation for each genotyping platform was performed separately and then combined. The final set of genotype data included 30,022,375 and 26,079,446 genetic variants for AA and EA, respectively. After removing genetic variants with MAF ≤ 0.01, imputation quality score (INFO score) ≤ 0.4 in any platform-based imputation, and indels, a total of 13,793,193 SNPs in AA and 7,727,215 SNPs in EA were available for analysis. We used the GENESIS package(28) in R to infer population structure in the analytic sample, and the PC-AiR function was used to extract the first five genotype PCs which were subsequently used to adjust for population structure.

medRxiv preprint doi: https://doi.org/10.1101/2024.01.03.24300768; this version posted January 5, 2024. The copyright holder for this preprint (which was not certified by peer review) is the author/funder, who has granted medRxiv a license to display the preprint in perpetuity. It is made available under a CC-BY-NC-ND 4.0 International license .

2.2.2. Gene Expression Data

Gene expression levels were measured from Epstein-Barr virus (EBV) transformed B-lymphoblastoid cell lines (LCLs) created from blood samples from a subset of GENOA AA (n=1,233) and EA (n=919). Gene expression levels of AA samples were measured using the Affymetrix Human Transcriptome Array 2.0, while gene expression levels of EA samples were measured using Affymetrix Human Exon 1.0 ST Array. We followed the procedures outlined by Shang et al.(18) In particular, the Affymetrix Expression Console was used for quality control and all array images passed visual inspection. In AA, 28 samples were removed due to either low signal-to-noise ratio (n=1), abnormal polyadenylated RNA spike-in controls (Lys < Phe < Thr < Dap; n=24), sample mislabeling (n=2), or low RNA integrity (n=1), resulting in a total of n=1,205 AA samples for analysis. In EA, duplicated samples (n=31), control samples (n=11) and sex mismatch samples (n=2) were removed, resulting in n=875 EA samples for analysis. We processed data in each population separately. Raw intensity data were processed using the Affymetrix Power Tool software (29). AffymetrixCEL files were normalized using the Robust Multichip Average (RMA) algorithm which included background correction, quantile normalization, $\log_2$-transformation, and probe set summarization.(30) The algorithm also includes GC correction (GCCN), signal space transformation (SST), and gain lock (value=0.75) to maintain linearity. The Brainarray custom CDF(31) v.19 was used to map the probes to genes. This custom CDF uses updated genomic annotations and multiple filtering steps to ensure that the probes used are specific for the intended gene cluster. Specifically, it removes probes with non-unique matching cDNA/EST sequences that can be assigned to more than one gene cluster. As a result, gene expression data processed using custom CDF are expected to be largely free of mappability issues. After mapping, ComBat(32) was used to remove batch effects. For each

medRxiv preprint doi: https://doi.org/10.1101/2024.01.03.24300768; this version posted January 5, 2024. The copyright holder for this preprint (which was not certified by peer review) is the author/funder, who has granted medRxiv a license to display the preprint in perpetuity. It is made available under a CC-BY-NC-ND 4.0 International license .

gene, we applied a linear regression model to adjust for age, sex, and first five genotype principal components (PCs). We then extracted the residuals and quantile normalized residuals across all samples. We analyzed a common set of 17,238 protein coding genes that were annotated in GENCODE (release 12) (33).

2.2.3. GWAS summary statistics

We used summary statistics from GWAS for general cognitive function (21), WMH (22), AD in EA(23), and AD in AA(24) as input for METRO. Three of the GWASs, Davies et al. (2018), Sargurupremraj et al. (2020), and Bellenguez et al. (2022), were selected because they are the largest meta-analyses to date with publicly available summary statistics; however, we note that all three were conducted in primarily EA samples. We also selected the Kunkle et al. (2021) GWAS because it is the largest meta-analysis to date with public available summary statistics in primarily AA samples. Below, we describe each GWAS and also provide information about the corresponding TWAS analyses that were reported in two of the input GWAS (WMH(22) and AD in EA(23)) which use the same GWAS summary statistics as our analysis but different gene expression data.

General cognitive function

We obtained GWAS summary statistics for general cognitive function from a meta-analysis by Davies et al. (2018) that includes the Cohorts for Heart and Aging Research in Genomic Epidemiology (CHARGE), the Cognitive Genomics Consortium (COGENT) consortia and the UK Biobank (UKB; Table 1) (21). This study included 300,486 EA individuals with ages between 16 and 102 years from 57 population-based cohorts. This is the largest available GWAS

medRxiv preprint doi: https://doi.org/10.1101/2024.01.03.24300768; this version posted January 5, 2024. The copyright holder for this preprint (which was not certified by peer review) is the author/funder, who has granted medRxiv a license to display the preprint in perpetuity. It is made available under a CC-BY-NC-ND 4.0 International license .

for general cognitive function, and there are currently no large-scale GWAS studies available in non-EA. General cognitive function was constructed from a number of cognitive tasks. Each cohort was required to have tasks that tested at least three different cognitive domains. Principal component (PC) analysis was performed on the cognitive tests scores within each cohort, and the first unrotated component was extracted as the measure of general cognitive function. Models performed within each cohort were adjusted for age, sex, and population stratification. Exclusion criteria included clinical stroke (including self-reported stroke) or prevalent dementia.

White matter hyperintensity

We obtained the GWAS summary statistics for WMH from a meta-analysis conducted by Sargurupremraj et al. (2020) that included 48,454 EA and 2,516 AA with mean age of 66.0 (SD=7.5) years from 23 population-based studies from the CHARGE consortium and UKB (Table 1) (22). We obtained publicly available GWAS summary statistics from only EA individuals. Summary statistics for only EA are publicly available for this GWAS. WMH was measured from MRI scans obtained from scanners with field strengths ranging from 1.5 to 3.0 Tesla and interpreted using a standardized protocol blinded to clinical or demographic features. In addition to T1 and T2 weighted scans, some cohorts included fluid-attenuated inversion recovery (FLAIR) and/or proton density (PD) sequences to measure WMH from cerebrospinal fluid. WMH volume measures were inverse normal transformed, and models adjusted for sex, age, genetic PCs and intracranial volume (ICV). Exclusion criteria included history of stroke or other pathologies that influence measurement of WMH at the time of MRI.

To functionally characterize and prioritize individual WMH genomic risk loci, Sargurupremraj et al.(22) (2020) conducted TWAS using TWAS-Fusion(34) with summary

medRxiv preprint doi: https://doi.org/10.1101/2024.01.03.24300768; this version posted January 5, 2024. The copyright holder for this preprint (which was not certified by peer review) is the author/funder, who has granted medRxiv a license to display the preprint in perpetuity. It is made available under a CC-BY-NC-ND 4.0 International license .

statistics from the WMH SNP-main effects (EA only) analysis and weights from gene expression reference panels from blood (Netherlands Twin Registry; Young Finns Study), arterial (Genotype-Tissue Expression, GTEx), brain (GTEx, CommonMind Consortium) and peripheral nerve tissue (GTEx). This study did not perform fine-mapping following TWAS analysis.

Alzheimer's disease (GWAS in EA)

We obtained the EA GWAS summary statistics for Alzheimer's disease from stage I meta-analysis by Bellenguez et al. (2022) that included EA from the European Alzheimer and Dementia Biobank (EADB), GR@ACE, EADI, GERAD/PERADES, DemGene, Bonn, the Rotterdam study, CCHS study, NxC and the UKB (Table 1) (23). The meta-analysis was performed on 39,106 clinically diagnosed AD cases, 46,828 proxy-AD and related dementia (ADD) cases, and 401,577 controls. AD cases were clinically diagnosed in all cohorts except UKB, where individuals were identified as proxy-ADD cases if their parents had dementia. Participants without the clinical diagnosis of AD, or those without any family history of dementia, were used as controls. Models performed within each cohort were adjusted for PCs and genotyping centers, when necessary.

To examine the downstream effects of new AD-associated variants on molecular phenotypes in various AD-relevant tissues, Bellenguez et al. (2022) conducted a TWAS with stage I AD GWAS results. The TWAS was performed by training functional expression and splicing reference panels based on the Accelerating Medicines Partnership (AMP)-AD bulk brain and EADB lymphoblastoid cell lines (LCL) cohorts, while leveraging pre-calculated reference panel weights(35) for the GTEx dataset(36) in tissues and cells of interest. TWAS associations were then fine-mapped using Fine-mapping Of CaUsal gene Sets (FOCUS) (37).

medRxiv preprint doi: https://doi.org/10.1101/2024.01.03.24300768; this version posted January 5, 2024. The copyright holder for this preprint (which was not certified by peer review) is the author/funder, who has granted medRxiv a license to display the preprint in perpetuity. It is made available under a CC-BY-NC-ND 4.0 International license .

Alzheimer's disease (GWAS in AA)

We also acquired the AA GWAS summary statistics for Alzheimer's disease from meta-analysis by Kunkle et al. (2021)(24) that included individuals of African American ancestry from 15 cohort studies from the AD Genetics Consortium (ADGC; Table 1). The meta-analysis was performed on 2,748 clinically diagnosed AD cases and 5,222 controls with a mean age of 74.2 years (SD=13.6). Models performed within each cohort were adjusted for age, sex, and PCs for population substructure.

2.3 Statistical Methods

2.3.1. Multi-ancestry transcriptome-wide association study

Using the Multi-ancEstry TRanscriptOme-wide analysis (METRO) (20), we conducted a high-powered TWAS with calibrated type I error control to identify the key gene-trait associations and transcriptomic mechanisms underlying general cognitive function, WMH and AD. Since gene expression prediction models constructed in different ancestries may contain complementary information, even when the input GWAS was conducted in a single ancestry (20), we used METRO to model gene expression from EA and AA simultaneously. METRO uses a joint-likelihood framework that accounts for SNP effect size heterogeneity and LD differences across ancestries. The framework selectively upweights information from the ancestry that has greater certainty in the gene expression prediction model, increasing power and allowing characterization of the relative contribution of each ancestry to the TWAS results.

METRO is described in Li et al.(20) Briefly, each gene is examined separately using gene expression data from M different genetic ancestries. $\boldsymbol{Z_m}$ is the n_m-vector of gene expression

medRxiv preprint doi: https://doi.org/10.1101/2024.01.03.24300768; this version posted January 5, 2024. The copyright holder for this preprint (which was not certified by peer review) is the author/funder, who has granted medRxiv a license to display the preprint in perpetuity. It is made available under a CC-BY-NC-ND 4.0 International license .

measurements on n_m individuals in the mth ancestry with $m \in \{1,\ldots,M\}$. For the gene of interest, all *cis*-SNPs (p), which are in potential linkage disequilibrium (LD) with each other, were extracted as predictors for gene expression. $\boldsymbol{G_m}$ is denoted as the $n_m \times p$ genotype matrix for these *cis*-SNPs. Besides the gene expression data, we also used GWAS summary statistics from n individuals for an outcome trait of interest. $\boldsymbol{\gamma}$ is the n-vector of outcome measurements in the GWAS data and $\boldsymbol{G}$ is the corresponding $n \times p$ genotype matrix on the same set of p *cis*-SNPs. The expression vector $\boldsymbol{z_m}$, the outcome vector $\boldsymbol{\gamma}$, and each column of the genotype matrixes are centered and standardized. $\boldsymbol{G_m}$ and $\boldsymbol{G}$ have a mean of zero and variance of one. For each TWAS, we used GWAS summary statistics in the form of marginal z-scores and a SNP-SNP correlation (LD) matrix estimated with genotype data from our GENOA sample that correspond with the ancestry of the GWAS (EA or AA). The following equations describe the relationships between the SNPs, gene expression and the outcome:

$$\boldsymbol{z}_m = \boldsymbol{G}_m \boldsymbol{\beta}_m + \boldsymbol{\epsilon}_m, \qquad \text{(Equation 1)}$$

$$\boldsymbol{\gamma} = \alpha(\boldsymbol{G}\boldsymbol{\beta}) + \boldsymbol{\epsilon}_y, \qquad \text{(Equation 2)}$$

Equation (1) describes the relationship between gene expression and the *cis*-SNP genotypes in the gene expression study in GENOA for the mth ancestry (EA or AA). β_m is a p vector of the *cis*-SNP effects on the gene expression in the mth ancestry and ε_m is an n_m-vector of residual errors with each element following an independent and normal distribution $N(0, \sigma^2_m)$ with an ancestry specific variance σ^2_m. Equation (2) describes the relationship between the genetically regulated gene expression (GReX), calculated from estimated SNP prediction weights, and the outcome trait (general cognitive function, WMH or AD) from the GWAS. There, $G\beta$ denotes an n-vector of GReX constructed for the GWAS individuals, where $\beta = \Sigma_m$

medRxiv preprint doi: https://doi.org/10.1101/2024.01.03.24300768; this version posted January 5, 2024. The copyright holder for this preprint (which was not certified by peer review) is the author/funder, who has granted medRxiv a license to display the preprint in perpetuity. It is made available under a CC-BY-NC-ND 4.0 International license .

$w_m\beta_m$ is a *p*-vector of SNP effects on the gene expression in the GWAS data, where the weights $\Sigma^{M}_{m=1} w_m=1$ and $w_m \geq 0$. The alpha value (α) is the effect of GReX constructed for the GWAS individuals on the outcome trait, and ε_y is an n_m-vector of residual errors with each element following an independent and normal distribution N(0, σ^2_m). Both equations, specified based on separate studies, are connected through the predictive SNP effects on the gene expression (β_m and β). A key assumption made is that the SNP effects on the gene expression in the GWAS, β, can be expressed as a weighted summation of the SNP effects on gene expression in the expression studies conducted across ancestries.

We derived the overall GReX effect α and the contribution weight of each ancestry (w_1 for AA and w_2 for EA) to infer the extent and contribution of the two genetic ancestries in informing the GReX-trait association. The joint model defined in Equations 1 and 2 allows us to borrow association strength across multiple ancestries to enable powerful inference of GReX-trait associations for general cognitive function, WMH and AD. We declared the gene to be significant if the p-value was below the corresponding Bonferroni corrected threshold for the number of tested genes ($P<0.05/17{,}238 = 2.90\times10^{-6}$). Manhattan plots and quantile-quantile (QQ) plots were generated using the *qqman*(38) R package.

2.3.2 Fine-mapping analysis

Since genes residing in the same genomic region may share eQTLs or contain eQTL SNPs in LD with each other, TWAS test statistics for genes in the same region can be highly correlated, making it difficult to identify the true biologically relevant genes among them. To prioritize the putatively causal genes identified by METRO for general cognitive function, WMH, and AD, we conducted TWAS fine-mapping using FOCUS (Fine-mapping Of CaUsal

medRxiv preprint doi: https://doi.org/10.1101/2024.01.03.24300768; this version posted January 5, 2024. The copyright holder for this preprint (which was not certified by peer review) is the author/funder, who has granted medRxiv a license to display the preprint in perpetuity. It is made available under a CC-BY-NC-ND 4.0 International license .

gene Sets) (37). To identify a genomic region with at least one significant gene detected by METRO, we obtained a set of independent, non-overlapping genomic regions, or LD blocks, using Ldetect (39). In each analyzed genomic block, using a standard Bayesian approach, we assigned a posterior inclusion probability (PIP) for each gene to be causal, given the observed TWAS statistics. We used gene-level Z scores, created from p-values using the inverse cumulative distribution function (CDF) of a standard normal distribution, as input into FOCUS. We then ranked the PIPs and computed the 90%-credible set that contains the causal gene with 90% probability. In the FOCUS analysis, a null model which assumes none of the genes in the region are causally associated with the trait is also considered as a possible outcome and may be included in the credible set. Through fine-mapping, we narrowed down significantly associated genes identified by METRO to a shorter list of putatively true associations.

2.3.3 Characterization of identified genes

To interpret our TWAS findings, both before and after fine-mapping, we further examined whether the genes identified by METRO overlapped with those previously identified by their corresponding input GWAS. We created a set of Venn diagrams of overlapping genes identified using METRO with those from the SNP-based GWAS association results(21–24) mapped to the nearest gene using the *VennDiagram* R package (40). We then constructed a second set of Venn diagrams showing overlapping genes identified using METRO with genes identified by gene-based association analyses in each of the input GWAS studies. The gene-based analyses were conducted using MAGMA(41) (general cognitive function,(21) WMH(22), and AD (AA GWAS)(24)) or gene prioritization tests (AD (EA GWAS)(23)). Finally, we created a set of Venn diagrams comparing genes identified using METRO with those identified

medRxiv preprint doi: https://doi.org/10.1101/2024.01.03.24300768; this version posted January 5, 2024. The copyright holder for this preprint (which was not certified by peer review) is the author/funder, who has granted medRxiv a license to display the preprint in perpetuity. It is made available under a CC-BY-NC-ND 4.0 International license .

in the TWAS that were conducted as part of the WMH(22) and AD (EA GWAS)(23) input GWAS studies. We used the *geneSynonym* R package(42) to ensure that genes named differently across studies were captured.

2.3.4 Functional Enrichment Analysis

To characterize the biological function of the identified genes by METRO for general cognitive function, WMH and AD, we performed gene set enrichment analysis. Specifically, we used the g:GOSt(43) tool on the web software g:Profiler and mapped the genes to known functional informational sources, including Gene Ontology (GO): molecular function (MF), GO: biological process (BP), GO: cellular component (CC), Kyoto Encyclopedia of Genes and Genomes (KEGG), Reactome (REAC), WikiPathways (WP), Transfac (TF), MiRTarBase (MIRNA), Human Protein Atlas (HPA), CORUM protein complexes, and Human Phenotype Ontology (HP). In this analysis, we used the default option g:SCS method (Set Counts and Sizes) in g:Profiler for multiple testing correction and presented pathways identified with an adjusted p-value < 0.05. Driver terms in GO are highlighted using a two-stage algorithm for filtering GO enrichment results, providing a more efficient and reliable approach compared to traditional clustering methods. This feature groups significant terms into sub-ontologies based on their relations, and the second stage identifies leading gene sets that give rise to other significant functions in the same group of terms. This method uses a greedy search strategy that recalculates hypergeometric p-values and results in the consideration of multiple leading terms in a component, rather than selection of terms with the highest significance level.

Results

medRxiv preprint doi: https://doi.org/10.1101/2024.01.03.24300768; this version posted January 5, 2024. The copyright holder for this preprint (which was not certified by peer review) is the author/funder, who has granted medRxiv a license to display the preprint in perpetuity. It is made available under a CC-BY-NC-ND 4.0 International license .

In Table 1, we provide descriptive statistics for the samples used in the eQTL mapping study (e.g., 1,032 AA and 801 EA from GENOA) and the four input GWAS.(21–23) The GENOA eQTL study included participants with a mean age of 56.9 (SD=10.0) years. More than half of participants were female (65.6%). Mean age of participants was 56.9 (SD=7.8) years in the general cognitive function GWAS(21), and 64.2 years in the WMH GWAS.(22) In the AD GWAS in EA (23), mean age was 73.6 (SD=8.1) years for cases and 67.9 (SD=8.6) years for controls. In the AD GWAS in AA (24), mean age was 74.2 (SD=13.6) years for all participants.

Using METRO, we identified 602 genes associated with general cognitive function, 45 genes associated with WMH, 231 genes associated with AD (EA GWAS), and 9 genes associated with AD (AA GWAS) that were significant at the Bonferroni corrected alpha level ($P<2.90x10^{-6}$; Figure 1, Tables S1-3). Genomic inflation factors for the TWAS p-values ranged from 1.00 to 2.55 (Figure 2). Among the three neurocognitive outcomes, prior to fine-mapping, METRO TWAS identified the *ICA1L* gene overlapping between WMH and AD (from EA GWAS); the *FMNL1* gene overlapping between WMH and general cognitive function; and 22 genes enriched in AD-related pathways and functions overlapping between general cognitive function and AD (from EA GWAs) (Figure 3a; Figure S1). After fine-mapping, the only overlapping gene that remained was *ICA1L* between WMH and AD (Figure 3b). The METRO TWAS for AD (AA GWAS) identified 9 genes overlapping with those identified in AD (EA GWAS); however, following fine-mapping, only *TOMM40* overlapped between the two AD TWASs (Figure 3b).

For all identified genes, we also examined the contribution weights of expression prediction models for the EA and AA ancestries, prior to fine-mapping ($P<2.90x10^{-6}$; Figure 4). For the WMH TWAS, we found that a large proportion of genes had stronger contributions from

medRxiv preprint doi: https://doi.org/10.1101/2024.01.03.24300768; this version posted January 5, 2024. The copyright holder for this preprint (which was not certified by peer review) is the author/funder, who has granted medRxiv a license to display the preprint in perpetuity. It is made available under a CC-BY-NC-ND 4.0 International license .

EA weights than AA weights (65.2%). This is consistent with Li et al. (2022)(20) who found that the gene expression prediction models constructed in the same ancestry as the input GWAS, in this case EA, often have larger contribution weights than those constructed in other ancestries. However, for both general cognitive function and AD (EA and AA GWAS), the contributions from EA and AA weights were similar, which likely increased power to identify genes relevant to AA.

After fine-mapping, there were 266 genes in the 90%-credible set across 172 different genomic regions for general cognitive function. This gene set included 82 genes that were not previously identified in the SNP-based GWAS results (mapped to the nearest gene) or the gene-based analysis results from Davies et al. (2018)(21) (Figure 5, Table S1); however, it is likely that some of these genes are in broader genomic regions tagged by the GWAS-identified SNPs. Specifically, there were 126 and 168 overlapping genes between METRO and the SNP-based and gene-based associations from Davies et al. (2018)(21), respectively (Figure 5). The 266 METRO-identified genes were enriched in regulatory pathways involved in protein binding ($p_{adj} = 1.17 \times 10^{-5}$), developmental cell growth ($p_{adj} = 3.33 \times 10^{-5}$), and protein metabolic process ($p_{adj} = 7.18 \times 10^{-4}$), as well as neurodevelopmental processes such as neuron to neuron synapse ($p_{adj} = 1.22 \times 10^{-3}$) and neuron projection ($p_{adj} = 7.14 \times 10^{-3}$; Figure 6). The 82 genes that were not previously identified in Davies et al. (2018)(21) were enriched for positive regulation of biological process ($p_{adj} = 1.77 \times 10^{-2}$), proteasome activator complex ($p_{adj} = 1.00 \times 10^{-2}$), nucleoplasm ($p_{adj} = 1.29 \times 10^{-2}$) and chromatin ($p_{adj} = 4.71 \times 10^{-5}$; Figure S2).

After fine-mapping, there were 23 genes in the 90%-credible set across 15 genomic regions for WMH, including 12 genes that were not previously identified in the SNP-based GWAS results mapped to the nearest gene or the gene-based analysis results from

medRxiv preprint doi: https://doi.org/10.1101/2024.01.03.24300768; this version posted January 5, 2024. The copyright holder for this preprint (which was not certified by peer review) is the author/funder, who has granted medRxiv a license to display the preprint in perpetuity. It is made available under a CC-BY-NC-ND 4.0 International license .

Sargurupremraj et al. (2020)(22) (Figure 7, Table S2). Specifically, there were 7 and 12 overlapping genes between METRO and the SNP-based and gene-based associations from Sargurupremraj et al. (2020)(22), respectively (Figure 7). The 23 METRO-identified genes were enriched for zinc finger motif ($p_{adj} = 1.27 \times 10^{-2}$), miRNA has-212-5p ($p_{adj} = 1.94 \times 10^{-2}$) and retinal inner plexiform layer ($p_{adj} = 3.86 \times 10^{-2}$; Figure 8). The 12 genes associated with WMH that were previously not identified by Sargurupremraj et al. (2020)(22) were enriched for DNA binding domain Zinc Finger Protein 690 (ZNF690; $p_{adj} = 2.52 \times 10^{-3}$) and ClpX protein degradation complex ($p_{adj} = 4.97 \times 10^{-2}$; Figure S3).

After fine-mapping, there were 69 genes in the 90%-credible set across 56 genomic regions associated with AD (EA GWAS), including 45 genes that were not previously identified in the SNP-based GWAS results mapped to the nearest gene or the gene prioritization analysis results from Bellenguez et al. (2022)(23) (Figure 9, Table S3). Specifically, there were 16 and 14 overlapping genes between METRO and the SNP-based and gene prioritization test results from Bellenguez et al. (2022)(23), respectively (Figure 9). The 69 METRO-identified genes were enriched for AD-associated processes including regulation of amyloid fibril formation ($p_{adj} = 1.87 \times 10^{-3}$), amyloid-beta clearance ($p_{adj} = 1.90 \times 10^{-3}$), microglial cell activation ($p_{adj} = 5.79 \times 10^{-3}$), amyloid-beta metabolic process ($p_{adj} = 1.07 \times 10^{-2}$), and neurofibrillary tangle ($p_{adj} = 2.80 \times 10^{-4}$; Figure 10). The 45 genes associated with AD that were previously not identified by Bellenguez et al. (2022)(23) were enriched for hematopoietic cell lineage ($p_{adj} = 1.73 \times 10^{-3}$) and neurofibrillary tangle ($p_{adj} = 9.13 \times 10^{-3}$; Figure S4).

We identified 2 genes, *APOE* and *PVRL2*, in the 90%-credible set associated with AD (AA GWAS) (Table S4). After fine-mapping, none of these genes overlapped with SNP-based GWAS results mapped to the nearest gene or the gene-based analysis results from Kunkle et al.

medRxiv preprint doi: https://doi.org/10.1101/2024.01.03.24300768; this version posted January 5, 2024. The copyright holder for this preprint (which was not certified by peer review) is the author/funder, who has granted medRxiv a license to display the preprint in perpetuity. It is made available under a CC-BY-NC-ND 4.0 International license .

(2021), since they are both in the broader *APOE* region, which was the only identified gene in Kunkle et al (2021). The 2 METRO-identified genes were enriched for coreceptor-mediated virion attachment to host ($p_{adj} = 4.96 \times 10^{-2}$; Figure 11).

We compared the genes identified by METRO before and after fine-mapping with those identified by TWAS studies in Sargurupremraj et al. (2020)(22) and Bellenguez et al. (2022)(23) which used TWAS-Fusion (Figure 12). For WMH, there were 16 and 10 genes identified both by METRO before and after fine-mapping and by the TWAS-Fusion analysis conducted by Sargurupremraj et al. (2020)(22), respectively (Table 2). For AD, there were 24 and 10 genes identified both by METRO before and after fine-mapping and by the TWAS-Fusion followed by FOCUS fine-mapping analysis conducted by Bellenguez et al. (2022)(23) (Table 3). *ICA1L* was the only gene overlapping between all four AD and WMH TWAS association results.

Discussion

While previous studies have identified genes associated with cognitive function, WMH, and AD, there are few TWAS that utilize genetic and gene expression data from multiple ancestries to elucidate gene-trait associations and molecular mechanisms underlying the etiologies of cognitive function and neurocognitive disorders. Using the METRO method in GWAS consisting primarily of EA followed by FOCUS fine-mapping, we identified 266, 23, and 69 genes associated with general cognitive function, WMH, and AD, respectively, with 82, 12 and 45 of them not previously identified in the original GWAS. In addition, using an AA GWAS, we identified 2 fine-mapped genes associated with AD, both of which are proximal to *APOE*. Studying the transcriptomic mechanisms underlying cognitive function, WMH and dementia using both EA and AA expression data may enhance our understanding of cognitive

medRxiv preprint doi: https://doi.org/10.1101/2024.01.03.24300768; this version posted January 5, 2024. The copyright holder for this preprint (which was not certified by peer review) is the author/funder, who has granted medRxiv a license to display the preprint in perpetuity. It is made available under a CC-BY-NC-ND 4.0 International license .

health prior to and following the onset of dementia and further allow us to generalize findings from large scale EA GWAS to other ancestries.

AD and SVD have overlapping features that contribute to dementia neuropathology including breakdown of the blood-brain barrier(44) and the presence of small cortical and subcortical infarcts, microbleeds, perivascular spacing, and WMH in brain tissue(45). After fine-mapping, Islet Cell Autoantigen 1 Like (*ICA1L*) was identified in both the WMH and AD TWAS. This is as a highly plausible prioritized gene that is likely to modulate the metabolism of amyloid precursor protein (APP)(23) and increase risk of AD. *ICA1L* encodes a protein whose expression is activated by type IV collagen and plays a crucial role in myelination(46). Increased *ICA1L* expression is also associated with lower risk of AD(47–49) and small vessel strokes (SVS), the acute outcomes of cerebral SVD, which may lead to VaD(50). Consistent with these studies, our TWAS found that decreased expression of *ICA1L* is associated with increased risk of AD and WMH, a subclinical indicator of SVD. Single-cell RNA-sequencing has shown *ICA1L* expression to be enriched in cortical glutamatergic excitatory neurons, which are crucial components in neural development and neuropathology through their role in cell proliferation, differentiation, survival, neural network formation and cell death(51,52). *ICA1L* has been examined as a possible drug target for SVD, AD, and other neurodegenerative diseases(50,53); however, it is not recommended as a prioritized drug at this time due to potential side effects including increased risk of coronary artery disease and myocardial infarction as well as lower diastolic blood pressure(53). Nevertheless, *ICA1L* may contribute to overlapping AD and VaD neuropathology, and it could be a potential target for therapeutics and/or preventative treatments for AD and VaD in the future if adverse events can be reduced.

medRxiv preprint doi: https://doi.org/10.1101/2024.01.03.24300768; this version posted January 5, 2024. The copyright holder for this preprint (which was not certified by peer review) is the author/funder, who has granted medRxiv a license to display the preprint in perpetuity. It is made available under a CC-BY-NC-ND 4.0 International license .

Our TWAS of AD (from EA GWAS) identified 45 genes that were not identified in the SNP-based GWAS results mapped to the nearest gene or the gene-based analysis reported in Bellenguez et al. (2022)(23). The 45 genes were enriched for hematopoietic cell lineage, which are progenitors of red and white blood cells including those related to immunity (e.g., natural killer cells, T- and B- lymphocytes and other types of leukocytes)(54–60). Our TWAS identified genes that have been previously associated with AD, including *APOE, TOMM40, APOC4, CLU, PICALM* and *CR2,* among others(23,61,62). While we identified *APOE,* the strongest genetic risk factor for AD in most populations, after fine-mapping, we did not identify *ABCA7* which confers an equal or even greater risk for AD in AA(63–65). This finding is perhaps not surprising considering that our TWAS was conducted using an EA GWAS, and the strength of association between *ABCA7* and AD is comparatively weaker in EA than in AA.(65) To identify genes associated with AD risk in AA populations, specifically, it would be beneficial to perform a TWAS utilizing a well-powered AD GWAS in AA.

Our TWAS of AD (from AA GWAS) (24) identified only *TOMM40* and *PVRL2*, both proximal to *APOE*. *TOMM40* was also identified in our TWAS of AD (from EA GWAS), as well as other AD GWAS (23,61,62). *PVRL2* has been associated with metabolic syndrome, diabetic dyslipidemia, and AD(66,67). One study found that polymorphisms in *PVRL2* interact with variants in *TOMM40* to increase AD risk through pathways related to amyloid-beta metabolism in older Chinese adults(67). As larger AD GWAS in AA become available, we may be able to identify additional genes associated with disease while leveraging transcriptomic data from EA and AA.

In our AD EA TWAS, we also identified genes associated with other neurological and autoimmune diseases including Parkinson's disease (*CYB561*(68) and *SLC25A39*(69)), Crohn's

medRxiv preprint doi: https://doi.org/10.1101/2024.01.03.24300768; this version posted January 5, 2024. The copyright holder for this preprint (which was not certified by peer review) is the author/funder, who has granted medRxiv a license to display the preprint in perpetuity. It is made available under a CC-BY-NC-ND 4.0 International license .

disease (*ATG16L1*(70)), Amyotrophic lateral sclerosis (*SIGLEC9*(71)), and Riboflavin Transport Deficiency (*SLC52A1*(72)). These diseases have in common the progressive peripheral and cranial degeneration of neurons that impact processes such as voluntary muscle movement, vision, hearing and sensation. Although not explicitly identified in Bellenguez et al. (2022)(23), we also identified genes that were associated with AD in other studies including *RIN3* that is implicated in tau-mediated pathology, the *MS4A* (*4A* and *6A*) locus associated with mast cell activation, *TP53INP1* and *ZYX* that have been linked to myeloid enhancer activity(73), and *APOC4*, which is located proximal to *APOE*(74). We also identified additional genes involved in B cell autoimmunity (*HLA-DQA2*(75,76) and *CSTF1*(77)), neurodegenerative processes (*SUPT4H1*(78), *C6orf10*(79), *IKZF1*(80), and *DEDD*(81)), and neuronal growth (*IKZF1*(80) and *STYX*(82)). Our findings support the hypothesis that chronic activation of immune cells resident in the brain and peripheral nervous system appear to play a critical role in neuroinflammatory responses that drive the progression of neurodegeneration in AD.(83) Further, consistent with findings that AD and VaD often co-exist, our AD TWAS identified genes that were associated with lacunar and ischemic strokes as well as cerebral small vessel disease in other studies, including *SLC39A13*(84), *RAPSN*(84), *MAF1*(85), and *MME*(86,87).

Although our WMH TWAS identified 12 genes that were not included in the SNP-based GWAS results mapped to the nearest gene or the gene-based analysis reported in Sargurupremraj et al. (2020)(22), other studies found associations between *MAP1LC3B*(88), *ARMS2*(89,90) and *HTRA1*(84) with ischemic stroke, lacunar stroke, and cerebral SVD. The WMH TWAS also identified genes associated with AD (*ARMS2*)(91), atrial fibrillation (*NEURL*(92) and *GJC1*(93)), innate immunity (*EFTUD2*(94)) and apoptosis and neurodevelopment (*PDCD7*(95), *FBXO31*(96), and *ClpX*(97)). The 12 unique genes identified for WMH were enriched for DNA

medRxiv preprint doi: https://doi.org/10.1101/2024.01.03.24300768; this version posted January 5, 2024. The copyright holder for this preprint (which was not certified by peer review) is the author/funder, who has granted medRxiv a license to display the preprint in perpetuity. It is made available under a CC-BY-NC-ND 4.0 International license .

binding domain Zinc Finger Protein 690(98), which plays an essential role in gene regulation, transcription and various cellular processes, and ClpX protein degradation complex(99), which maintains protein homeostasis. Our findings were consistent with studies that showed neuroinflammation to be an immunological cascade reaction by glial cells of the central nervous system where innate immunity resides.

While our TWAS for general cognitive function did not show overlapping genes between the TWAS for AD and VaD, we identified genes associated with general cognitive function that were not explicitly identified by Davies et al. (2018)(21) which were associated with pre-clinical AD and VaD risk factors including cardiovascular diseases, immunity and Alzheimer's neuropathology. Our TWAS also identified genes previously associated with cognitive domains, neuropathology, and psychiatric illness including reading-related skills and neural structures (*SEMA6D*(100) and *SETBP1*(101)), working memory tasks (*CDH13*(102)) and Schizophrenia (*HP*(103,104), *C18orf1*(105) and *TMEM180*(106)). There are likely also distinct transcriptomic mechanisms that differentiate cognitive function and normal age-related brain changes from pathways related to dementia. Individuals who never develop dementia or significant cognitive decline still experience brain deterioration in normal aging that includes gray and white matter loss and ventricular enlargement which is accompanied by memory decline(107). Further, previous GWAS for general cognitive function and AD have shown few overlapping loci(21,108). In addition, studies of older individuals who are cognitively "resilient" with intact cognitive function, despite the presence of AD neuropathology, have found the genetic architecture of cognitive resilience to be distinct from that of AD(109). As such, relatively little is known about the pathways underlying cognitive aging in those without dementia. Thus,

medRxiv preprint doi: https://doi.org/10.1101/2024.01.03.24300768; this version posted January 5, 2024. The copyright holder for this preprint (which was not certified by peer review) is the author/funder, who has granted medRxiv a license to display the preprint in perpetuity. It is made available under a CC-BY-NC-ND 4.0 International license .

studying transcriptomic mechanisms that affect general cognitive function before development of dementia may shed light on cognitive aging without dementia.

We also compared genes identified by METRO after fine-mapping with those identified by TWAS-Fusion in Sargurupremraj et al. (2020)(22) and Bellenguez et al. (2022)(23). Among the 92 genes associated with WMH in Sargurupremraj et al. (2020)(22) and 23 genes identified by METRO, 10 genes overlapped. We note that the Sargurupremraj et al. (2020)(22) did not perform fine-mapping of their TWAS results, which is likely why we identified substantially fewer genes. There were also 10 overlapping genes among the 66 genes associated with AD in Bellenguez et al. (2022)(23) and 69 genes identified by METRO. For both TWAS comparisons, a relatively small number of genes overlap likely due to differences in eQTL prediction modeling. Sargurupremraj et al. (2020)(22) and Bellenguez et al. (2022)(23) used eQTL data from brain tissue, while we used eQTL data from transformed beta lymphocytes in blood tissue. While brain tissue is more relevant to WMH and AD phenotypes, blood cells do touch every cell bed that affects the brain, and are related to chronic inflammation, immunity, and oxidative stress, which are linked to cognitive performance and dementia. TWAS results from blood tissue in multiple ancestries provide complementary information to those reported in the GWAS.

Several limitations in the present study should be noted. First, our gene expression levels were measured using transformed B-lymphocytes from immortalized cell lines in GENOA. While transformed B-lymphocytes are a convenient source of DNA from blood tissue, we lack eQTL data for tissues that may be most relevant for AD and WMH (e.g., brain tissue, small brain vessels, and microglia). However, B-lymphocytes provide a unique and efficient way to examine the functional effects of genetic variations on gene expression that minimizes environmental influences(110). Second, METRO follows the standard TWAS approach of analyzing one gene

medRxiv preprint doi: https://doi.org/10.1101/2024.01.03.24300768; this version posted January 5, 2024. The copyright holder for this preprint (which was not certified by peer review) is the author/funder, who has granted medRxiv a license to display the preprint in perpetuity. It is made available under a CC-BY-NC-ND 4.0 International license .

at a time. Since genes residing in the same genomic region may share eQTLs or contain eQTL SNPs that are in LD with each other, the TWAS test statistics of genes in the same region may be highly correlated. To that end, it may be challenging to identify the truly biologically relevant genes among them(37,111). As such, we paired METRO with FOCUS to allow us to narrow down the list of potential causal genes for AD, VaD, and cognitive decline(37,112). Lastly, we primarily utilized EA GWAS that were publicly available with large sample sizes for general cognitive function, WMH, and AD. As expected, the gene expression prediction models constructed in the same ancestry as the GWAS (EA) tended to have larger contribution weights than AA. While we conducted a TWAS of AD in AA, the sample size of the AA GWAS likely did not allow us to properly power our TWAS. As such, a future direction would be to conduct TWAS of these traits using summary statistics from well-powered GWAS with AA ancestry or multiple ancestries as they become available.

Our study also has notable strengths. To our knowledge, our study is the first TWAS using expression mapping studies in multiple ancestries (EA and AA) to identify genes associated with cognitive function and neurocognitive disorders. By leveraging the complementary information in gene expression prediction models constructed in EA and AA, as well as the uncertainty in SNP prediction weights, we were able to conduct a highly powered TWAS to identify important gene-trait associations and transcriptomic mechanisms related to innate immunity, vascular dysfunction and neuroinflammation underlying AD, VaD, and general cognitive function. Using METRO, we were also able to estimate the ancestry contribution weights for specific genes and identify the extent to which a gene in EA or AA may contribute to the trait. However, it is noteworthy that the larger the contribution of the expression prediction models in the same ancestry as the GWAS (primarily EA, in this study) may allow for better

medRxiv preprint doi: https://doi.org/10.1101/2024.01.03.24300768; this version posted January 5, 2024. The copyright holder for this preprint (which was not certified by peer review) is the author/funder, who has granted medRxiv a license to display the preprint in perpetuity. It is made available under a CC-BY-NC-ND 4.0 International license .

predictive performance in the same ancestry. We also conducted FOCUS fine-mapping to narrow in on a list of putatively causal genes among multiple significant genes in a region. Our results suggest that there are similar pathways that contribute to healthy cognitive aging and progression of dementia, as well as distinct pathways that are unique to each neuropathology. By understanding overlapping and unique genes and transcriptomic mechanisms associated with each outcome, we may identify possible targets for prevention and/or treatments for cognitive aging and dementia.

Conclusion

In the present study, we conducted a multi-ancestry TWAS in EA and AA to identify genes associated with general cognitive function, WMH and AD. We identified genes associated with innate immunity, vascular dysfunction, and neuroinflammation. The WMH and AD TWAS also indicated that downregulation of *ICA1L* may contribute to overlapping AD and VaD neuropathology. To our knowledge, this study is the first TWAS analysis using expression mapping studies in multiple ancestries to identify genes associated with cognitive function and neurocognitive disorders, which may help to identify gene targets for pharmaceutical or preventative treatment for dementia.

medRxiv preprint doi: https://doi.org/10.1101/2024.01.03.24300768; this version posted January 5, 2024. The copyright holder for this preprint (which was not certified by peer review) is the author/funder, who has granted medRxiv a license to display the preprint in perpetuity. It is made available under a CC-BY-NC-ND 4.0 International license .

Author Contributions: Conceptualization, D.L.C., J.A.S.; methodology, D.L.C., J.A.S., X.Z.; software, formal analysis, and investigation, D.L.C., Z.L., L.S., S.M.R.; resources, T.H.M. and S.L.R.K.; writing—original draft preparation, D.L.C., J.A.S.; writing—review and editing, D.L.C., S.M.R., W.Z., T.H.M., S.L.R.K., X.Z., J.A.S.; visualization, D.L.C., Z.L.; supervision, J.A.S.; funding acquisition, S.L.R.K. and J.A.S. All authors have read and agreed to the published version of the manuscript.

Funding: Support for the Genetic Epidemiology Network of Arteriopathy (GENOA) was provided by the National Heart, Lung and Blood Institute (NHLBI, U01HL054457, RC1HL100185, R01HL087660, R01HL119443, R01HL133221) and the National Institute of Neurological Disorders and Stroke (NINDS, R01NS041558) of the NIH.

Informed Consent Statement: Written informed consent was obtained from all subjects involved in the study.

Data Availability Statement: The phenotype data and *APOE* genotypes used in the current study are available upon reasonable request to J.A.S. and S.L.R.K., and with a completed data use agreement (DUA). All other genotype data are available from the Database of Genotypes and Phenotypes (dbGaP): phs001401.v2.p1. Methylation and gene expression data are available from the Gene Expression Omnibus (GEO): GSE210256 and GSE138914. Due to IRB restriction, mapping of the sample IDs between genotype data (dbGaP) and methylation data (GEO) cannot be provided publicly, but is available upon written request to J.A.S. and S.L.R.K.

Acknowledgments: The authors wish to thank the staff and participants of the GENOA study.

Conflicts of Interest: The authors declare no conflict of interest.

medRxiv preprint doi: https://doi.org/10.1101/2024.01.03.24300768; this version posted January 5, 2024. The copyright holder for this preprint (which was not certified by peer review) is the author/funder, who has granted medRxiv a license to display the preprint in perpetuity. It is made available under a CC-BY-NC-ND 4.0 International license .

Table 1. Sample characteristics of expression quantitative trait locus (eQTL) mapping study and genome-wide association studies (GWAS) participants

eQTL mapping study: Genetic Epidemiology Network of Arteriopathy (GENOA)	
	Mean (SD) or N (%) or N
N	N=1833
Age (years)	56.85 (10.0)
Female	1202 (65.6%)
Race/Ethnicity	
African Americans	1032 (56.3%)
European Americans	801 (43.7%)

General cognitive function GWAS: CHARGE, COGENT, UKB[a] (Davies et al., 2018)	
	Mean (SD) or N (%) or N
N	300,486
Age (years)	56.91 (7.8)
Female	52.20%
Excluded for dementia and/or stroke diagnosis	N=4919

White matter hyperintensity (WMH) GWAS: CHARGE and UKB[a] (Sargurupremraj et al., 2020)	
	Mean (SD) or N (%) or N
N	48,454
Age (years)	64.17
Female	29215 (57.6%)
WMH volume (cm^3)	7.06 (8.8)
Excluded for stroke or pathologies	N=1572

EA Alzheimer's Disease (AD) GWAS: EADB, GR@ACE, EADI, GERAD/PERADES, DemGene, Bonn, the Rotterdam study, the CCHS study, NxC and the UKB[a] (Bellenguez et al., 2022)	
	Mean (SD) or N (%) or N
Discovery sample	
AD cases	N=39,106
AD proxy cases	N=46,828
Controls	N=401,577
Age (years)	
AD cases or proxy cases	73.55 (8.1)
controls	67.86 (8.6)
Female	
AD cases or proxy cases	62.90%
controls	56.10%

AA Alzheimer's Disease (AD) GWAS: AD Genetics Consortium[b] (Kunkle et al., 2021)	
	Mean (SD) or N (%) or N
N	7,970
AD cases	2,748 (34.5%)
controls	5,222 (65.5%)
Age (years)	74.2 (13.6)
Female	
AD cases	1,944 (69.8%)
controls	3,743 (71.7%)

Abbreviations: EA, European ancestry; AA, African ancestry

[a] GWAS include only European ancestry participants.

[b] GWAS includes only African ancestry participants.

medRxiv preprint doi: https://doi.org/10.1101/2024.01.03.24300768; this version posted January 5, 2024. The copyright holder for this preprint (which was not certified by peer review) is the author/funder, who has granted medRxiv a license to display the preprint in perpetuity. It is made available under a CC-BY-NC-ND 4.0 International license .

Table 2. Genes for WMH identified both by METRO followed by fine-mapping with FOCUS and by TWAS-Fusion conducted by Sargurupremraj et al. (2020)

Gene	ENSG	Chr	Start	End	Gene Name	Accession number
CALCRL	ENSG00000064989	2	188206691	188313187	calcitonin receptor like receptor	Source: HGNC Symbol; Acc: HGNC:1670
DCAKD	ENSG00000172992	17	43100706	43138499	dephospho-CoA kinase domain containing	Source: HGNC Symbol; Acc: HGNC: 2623
EFEMP1	ENSG00000115380	2	56093102	56151274	EGF containing fibulin extracellular matrix protein 1	Source: HGNC Symbol; Acc: HGNC: 3218
GJC1	ENSG00000182963	17	42875816	42908184	gap junction protein gamma 1	Source: HGNC Symbol; Acc: HGNC: 4280
ICA1L	ENSG00000163596	2	203637873	203736489	islet cell autoantigen 1 like	Source: HGNC Symbol; Acc: HGNC: 1444
KLHL24	ENSG00000114796	3	183353398	183402307	kelch like family member 24	Source: HGNC Symbol; Acc: HGNC: 2594
NBEAL1	ENSG00000144426	2	203879331	204091101	neurobeachin like 1	Source: HGNC Symbol; Acc: HGNC: 2068
NEURL	ENSG00000107954	10	105253462	105352303	neuralized E3 ubiquitin protein ligase 1	Source: HGNC Symbol; Acc: HGNC: 7761
NMT1	ENSG00000136448	17	43035360	43186384	N-myristoyltransferase 1	Source: HGNC Symbol; Acc: HGNC: 7857
WBP2	ENSG00000132471	17	73841780	73852588	WW domain binding protein 2	Source: HGNC Symbol; Acc: HGNC: 1273

Abbreviations: HGNC, Human Genome Organisation Gene Nomenclature Committee

medRxiv preprint doi: https://doi.org/10.1101/2024.01.03.24300768; this version posted January 5, 2024. The copyright holder for this preprint (which was not certified by peer review) is the author/funder, who has granted medRxiv a license to display the preprint in perpetuity. It is made available under a CC-BY-NC-ND 4.0 International license .

Table 3. Genes for AD identified both by METRO followed by fine-mapping with FOCUS and by TWAS-Fusion followed by fine-mapping with FOCUS conducted by Bellenguez et al. (2022)

Gene	ENSG	Chr	Start	End	Gene Name	Accession number
BLNK	ENSG00000095585	10	97948927	98031344	B cell linker	Source:HGNC Symbol;Acc:HGNC:14211
CPSF3	ENSG00000119203	2	9563780	9613230	cleavage and polyadenylation specific factor 3	Source:HGNC Symbol;Acc:HGNC:2326
DDX54	ENSG00000123064	12	113594978	113623284	DEAD-box helicase 54	Source:HGNC Symbol;Acc:HGNC:20084
GRN	ENSG00000030582	17	42422614	42430474	granulin precursor	Source:HGNC Symbol;Acc:HGNC:4601
ICA1L	ENSG00000163596	2	203637873	203736489	islet cell autoantigen 1 like	Source:HGNC Symbol;Acc:HGNC:14442
KLF16	ENSG00000129911	19	1852398	1863578	KLF transcription factor 16	Source:HGNC Symbol;Acc:HGNC:16857
LACTB	ENSG00000103642	15	63414032	63434260	lactamase beta	Source:HGNC Symbol;Acc:HGNC:16468
PPP4C	ENSG00000149923	16	30087299	30096697	protein phosphatase 4 catalytic subunit	Source:HGNC Symbol;Acc:HGNC:9319
SHARPIN	ENSG00000179526	8	145153536	145163027	SHANK associated RH domain interactor	Source:HGNC Symbol;Acc:HGNC:25321
TBX6	ENSG00000149922	16	30097114	30103245	T-box transcription factor 6	Source:HGNC Symbol;Acc:HGNC:11605

Abbreviations: HGNC, Human Genome Organisation Gene Nomenclature Committee

medRxiv preprint doi: https://doi.org/10.1101/2024.01.03.24300768; this version posted January 5, 2024. The copyright holder for this preprint (which was not certified by peer review) is the author/funder, who has granted medRxiv a license to display the preprint in perpetuity. It is made available under a CC-BY-NC-ND 4.0 International license .

(a) General cognitive function from Davies et al. (2018) GWAS

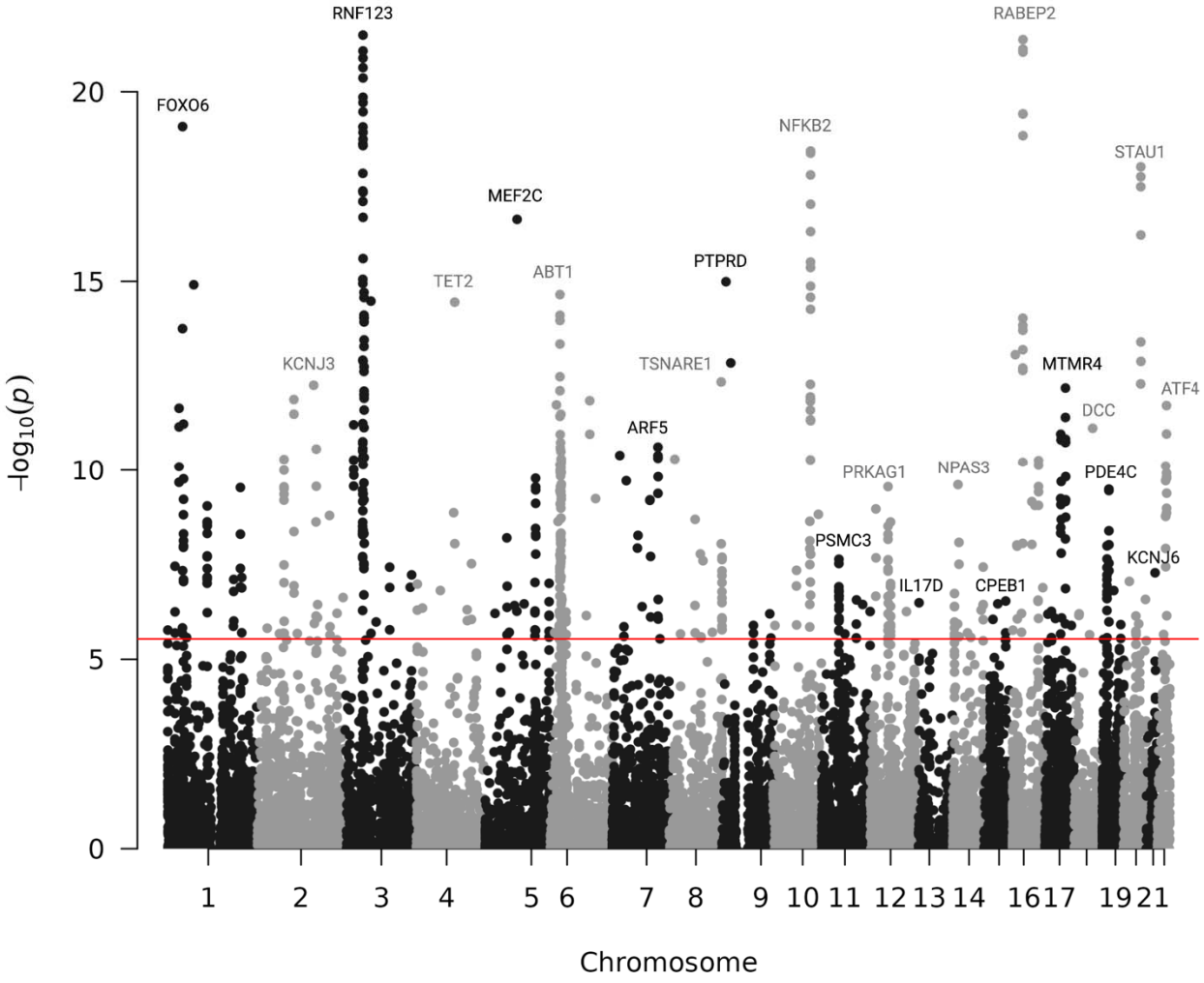

medRxiv preprint doi: https://doi.org/10.1101/2024.01.03.24300768; this version posted January 5, 2024. The copyright holder for this preprint (which was not certified by peer review) is the author/funder, who has granted medRxiv a license to display the preprint in perpetuity. It is made available under a CC-BY-NC-ND 4.0 International license .

(b) White matter hyperintensity from Sargurupremraj et al. (2020) GWAS

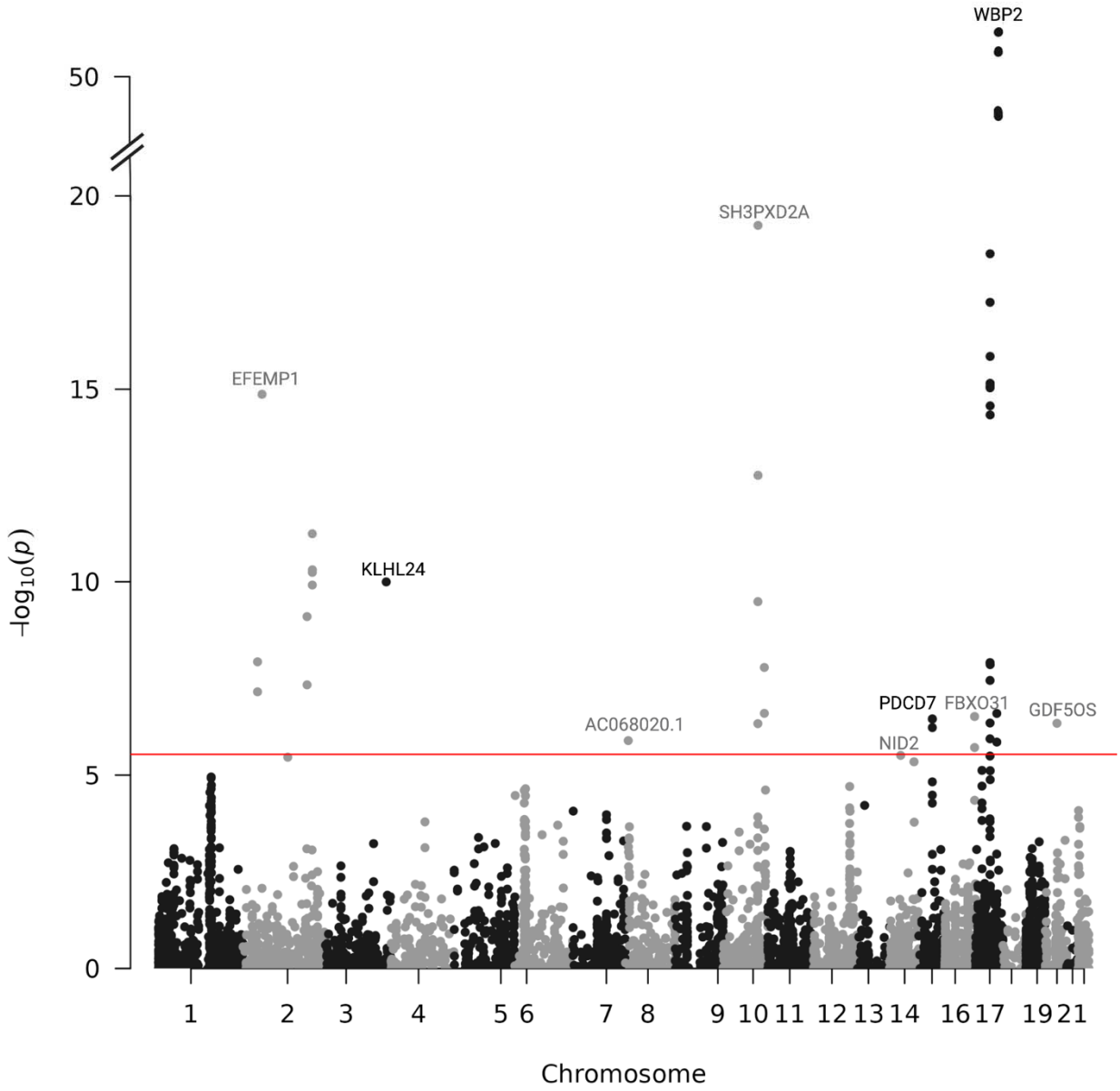

medRxiv preprint doi: https://doi.org/10.1101/2024.01.03.24300768; this version posted January 5, 2024. The copyright holder for this preprint (which was not certified by peer review) is the author/funder, who has granted medRxiv a license to display the preprint in perpetuity. It is made available under a CC-BY-NC-ND 4.0 International license .

(c) Alzheimer's Disease from Bellenguez et al. (2022) (EA GWAS sample)

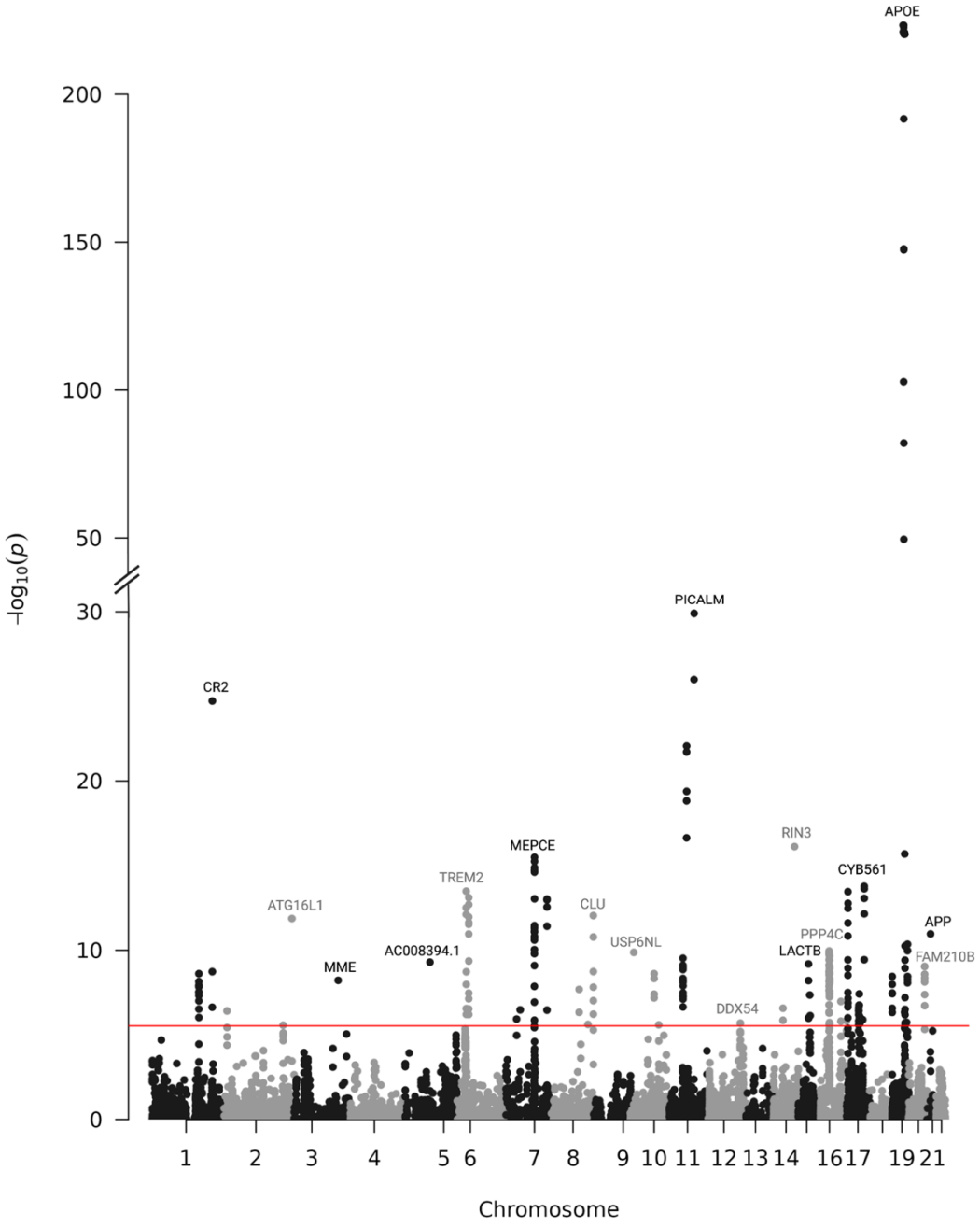

medRxiv preprint doi: https://doi.org/10.1101/2024.01.03.24300768; this version posted January 5, 2024. The copyright holder for this preprint (which was not certified by peer review) is the author/funder, who has granted medRxiv a license to display the preprint in perpetuity. It is made available under a CC-BY-NC-ND 4.0 International license .

(d) Alzheimer's Disease from Kunkle et al. (2021) (AA GWAS sample)

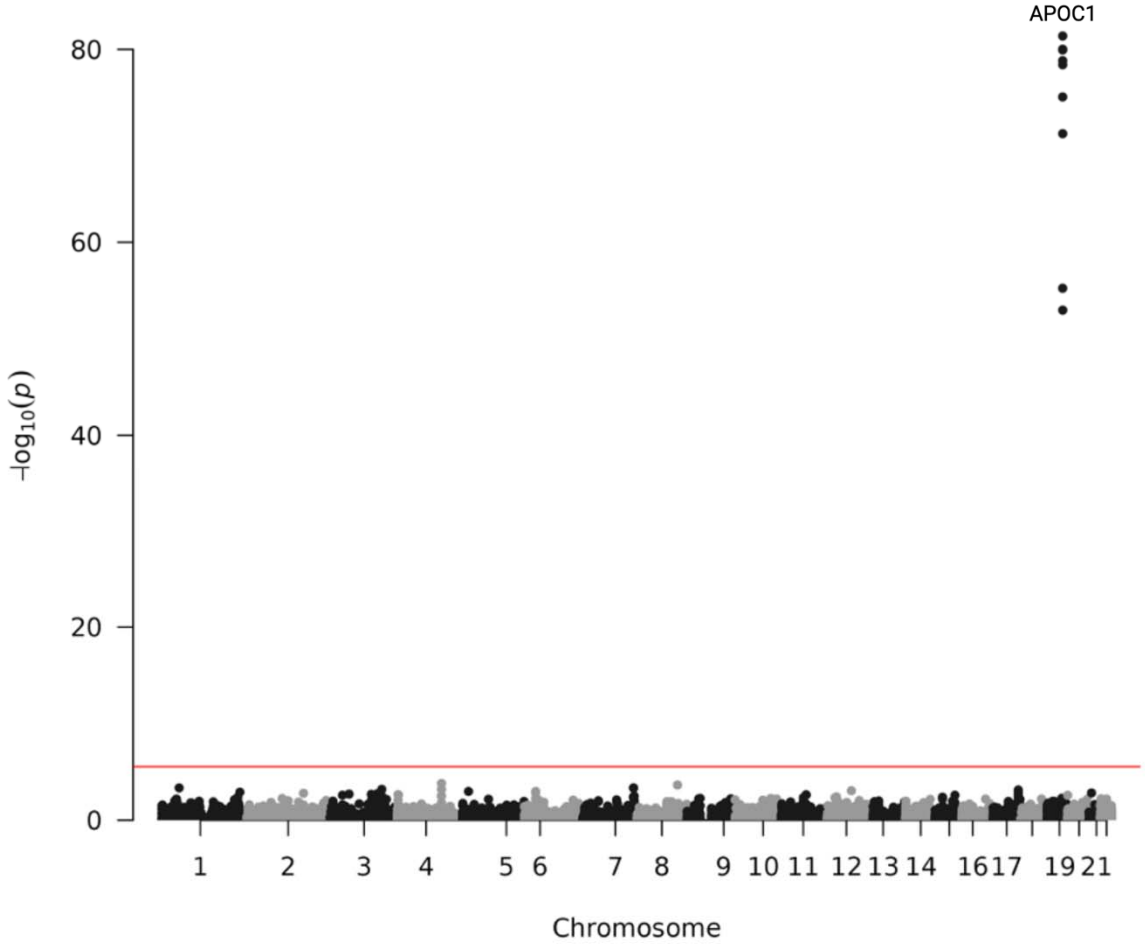

medRxiv preprint doi: https://doi.org/10.1101/2024.01.03.24300768; this version posted January 5, 2024. The copyright holder for this preprint (which was not certified by peer review) is the author/funder, who has granted medRxiv a license to display the preprint in perpetuity. It is made available under a CC-BY-NC-ND 4.0 International license .

Figure 1. Manhattan plots of -$\log_{10}$ p-values for gene-trait associations in METRO. Manhattan plots of the association between genes and (a) general cognitive function using summary statistics from Davies et al. (2018), (b) White matter hyperintensity from Sargurupremraj et al. (2020), (c) Alzheimer's disease from Bellenguez et al. (2022) (EA GWAS sample) and (d) Alzheimer's disease from Kunkle et al. (2021) (AA GWAS sample) using GENOA gene expression data. The red line indicates significance after Bonferroni correction ($P<2.90\times10^{-6}$).

medRxiv preprint doi: https://doi.org/10.1101/2024.01.03.24300768; this version posted January 5, 2024. The copyright holder for this preprint (which was not certified by peer review) is the author/funder, who has granted medRxiv a license to display the preprint in perpetuity. It is made available under a CC-BY-NC-ND 4.0 International license .

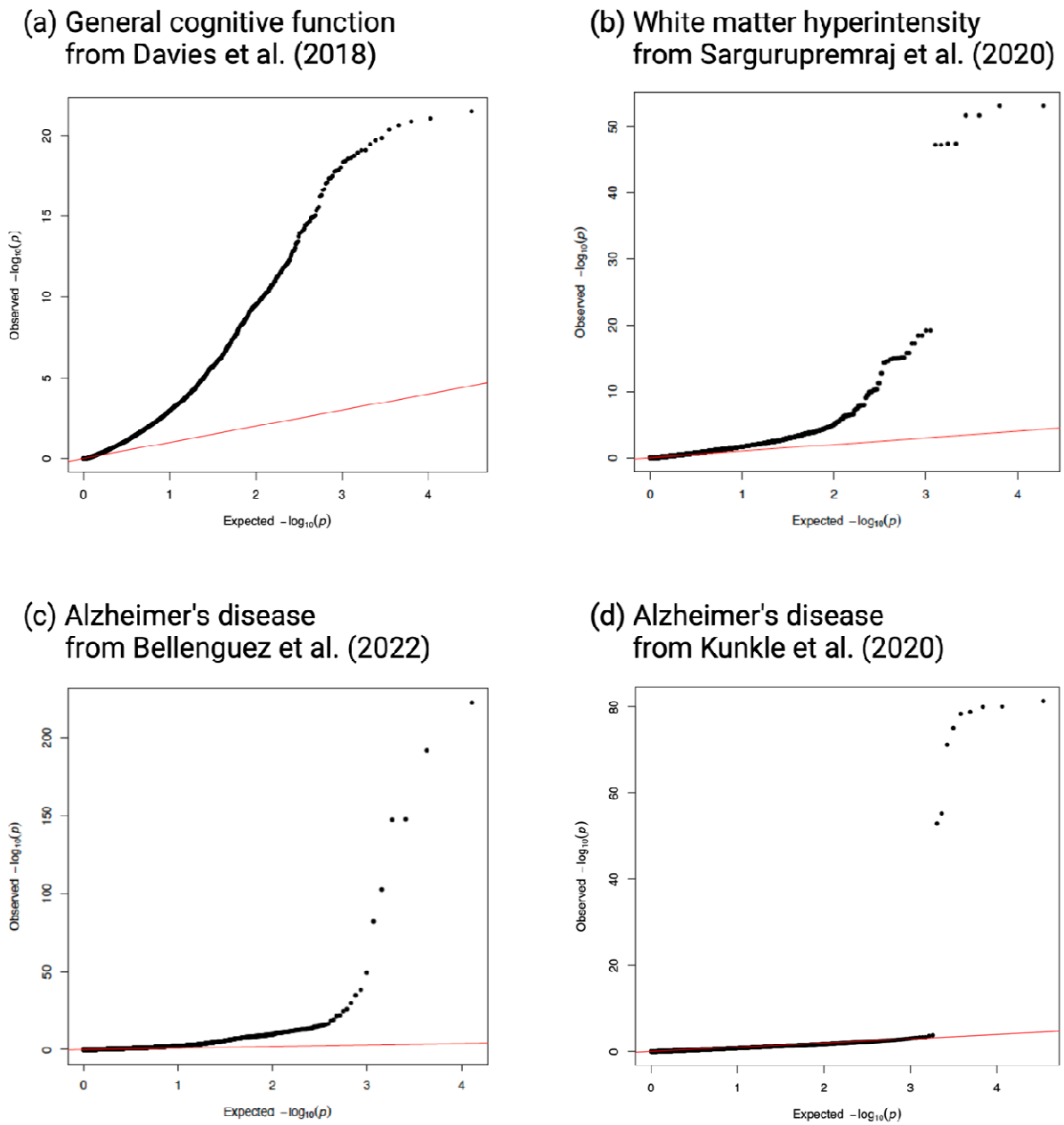

Figure 2. Quantile-quantile plots of -$\log_{10}$ p-values for gene-trait associations in METRO. Q-Q plots of the associations between genes and (a) general cognitive function (λ= 2.55) using summary statistics from Davies et al. (2018), (b) white matter hyperintensity (λ= 1.45) from Sargurupremraj et al. (2020), (c) Alzheimer's disease (λ= 2.09) from Bellenguez et al. (2022) (EA GWAS sample) and (d) Alzheimer's disease (λ= 1.0) from Kunkle et al. (2021)(AA GWAS sample) using GENOA gene expression data.

medRxiv preprint doi: https://doi.org/10.1101/2024.01.03.24300768; this version posted January 5, 2024. The copyright holder for this preprint (which was not certified by peer review) is the author/funder, who has granted medRxiv a license to display the preprint in perpetuity. It is made available under a CC-BY-NC-ND 4.0 International license .

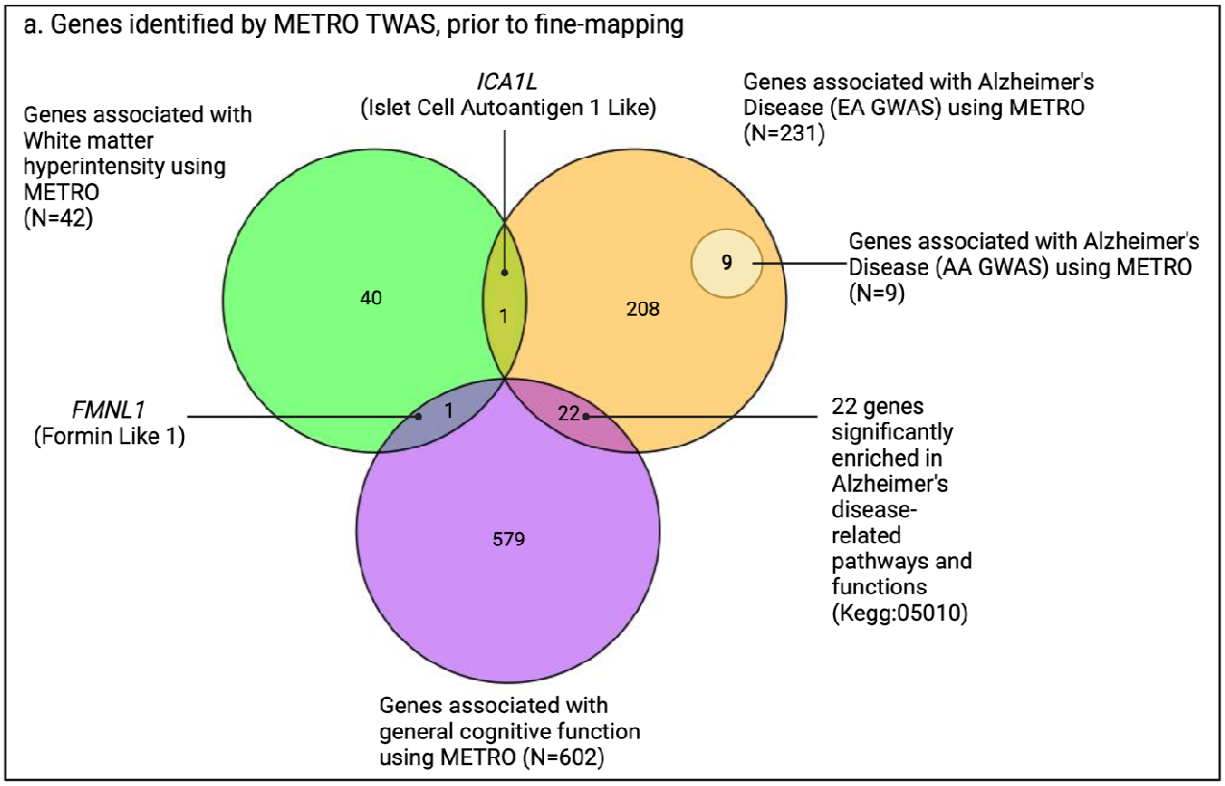

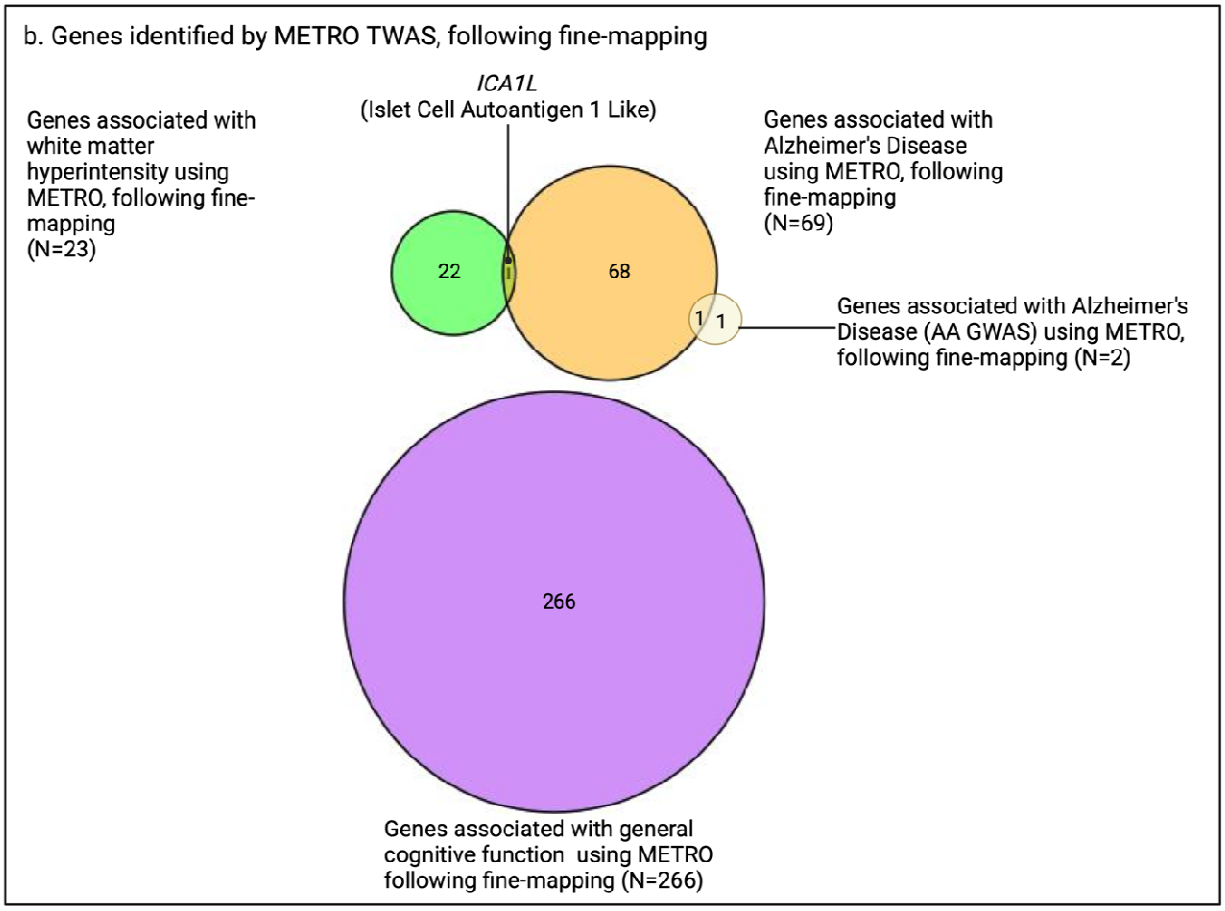

713

medRxiv preprint doi: https://doi.org/10.1101/2024.01.03.24300768; this version posted January 5, 2024. The copyright holder for this preprint (which was not certified by peer review) is the author/funder, who has granted medRxiv a license to display the preprint in perpetuity. It is made available under a CC-BY-NC-ND 4.0 International license .

Figure 3. Venn diagrams comparing number of genes associated with general cognitive function, white matter hyperintensity and Alzheimer's disease (AD) in European ancestry (EA) and AD in African ancestry (AA) using METRO, prior to and following FOCUS fine-mapping.

Venn diagrams comparing the number of genes associated with general cognitive function (purple; N=266 genes), white matter hyperintensity (WMH; green; N=23 genes) Alzheimer's disease (AD) in EA (orange; N=69 genes), and AD in AA (yellow; N=2 genes), (a) prior to fine-mapping and (b) following FOCUS(5) fine-mapping using METRO and GENOA expression data after Bonferroni correction ($P<2.90x10^{-6}$), with GWAS summary statistics obtained from the Davies et al. (2018), Sargurupremraj et al. (2020), Bellenguez et al. (2022), and Kunkle et al. (2021).

medRxiv preprint doi: https://doi.org/10.1101/2024.01.03.24300768; this version posted January 5, 2024. The copyright holder for this preprint (which was not certified by peer review) is the author/funder, who has granted medRxiv a license to display the preprint in perpetuity. It is made available under a CC-BY-NC-ND 4.0 International license .

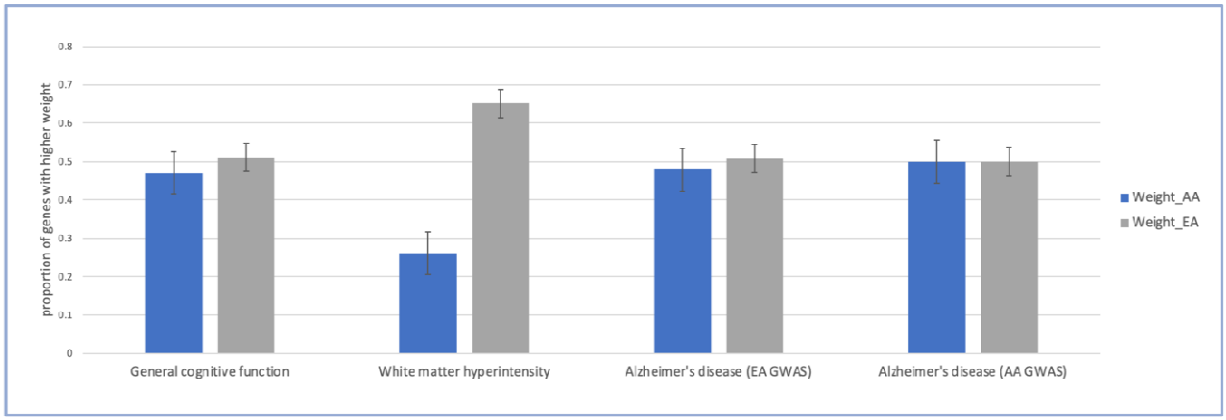

Figure 4. Contribution weights of expression prediction models across all significant fine-mapped genes identified by METRO.
Barplots of general cognitive function, white matter hyperintensity and Alzheimer's disease (AD) in European ancestry (EA) and AD in African ancestry (AA) comparing the proportion of significant genes with higher contribution weights of expression prediction models across all significant genes ($P<2.90x10^{-6}$). Black bars are the standard errors for the estimated proportions.

medRxiv preprint doi: https://doi.org/10.1101/2024.01.03.24300768; this version posted January 5, 2024. The copyright holder for this preprint (which was not certified by peer review) is the author/funder, who has granted medRxiv a license to display the preprint in perpetuity. It is made available under a CC-BY-NC-ND 4.0 International license .

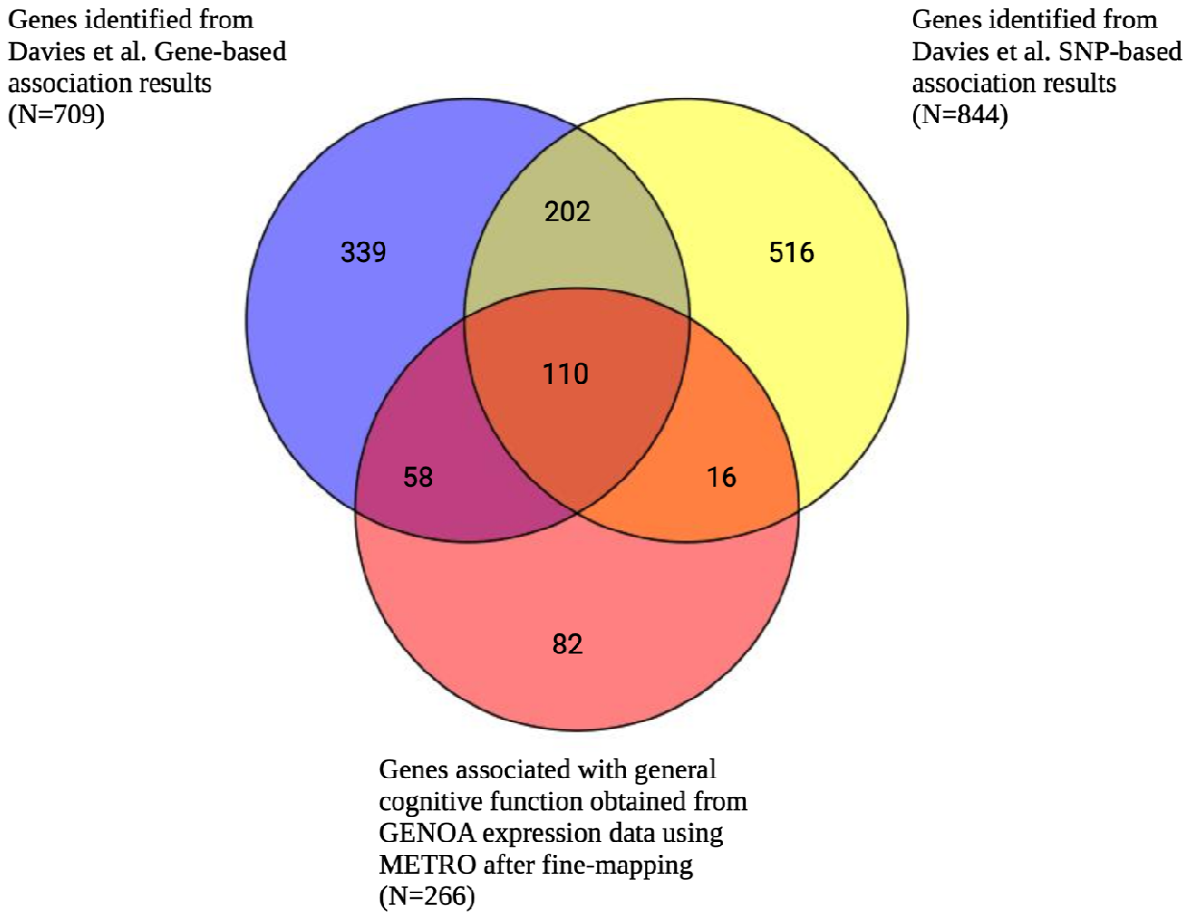

Figure 5. Venn diagram comparing number of METRO-identified genes associated with general cognitive function following FOCUS fine-mapping and genes identified by Davies et al. (2018) gene-based and SNP-based analyses.
Venn diagram comparing the number of genes associated with general cognitive function obtained from METRO using GENOA gene expression data after Bonferroni correction ($P<2.90x10^{-6}$) and FOCUS fine-mapping (red) and Davies et al. (2018). Davies et al. results included SNP-based association results that were mapped to the nearest gene ($P<5x10^{-8}$; yellow), and gene-based association results ($P<2.75x10^{-6}$; blue).

medRxiv preprint doi: https://doi.org/10.1101/2024.01.03.24300768; this version posted January 5, 2024. The copyright holder for this preprint (which was not certified by peer review) is the author/funder, who has granted medRxiv a license to display the preprint in perpetuity. It is made available under a CC-BY-NC-ND 4.0 International license .

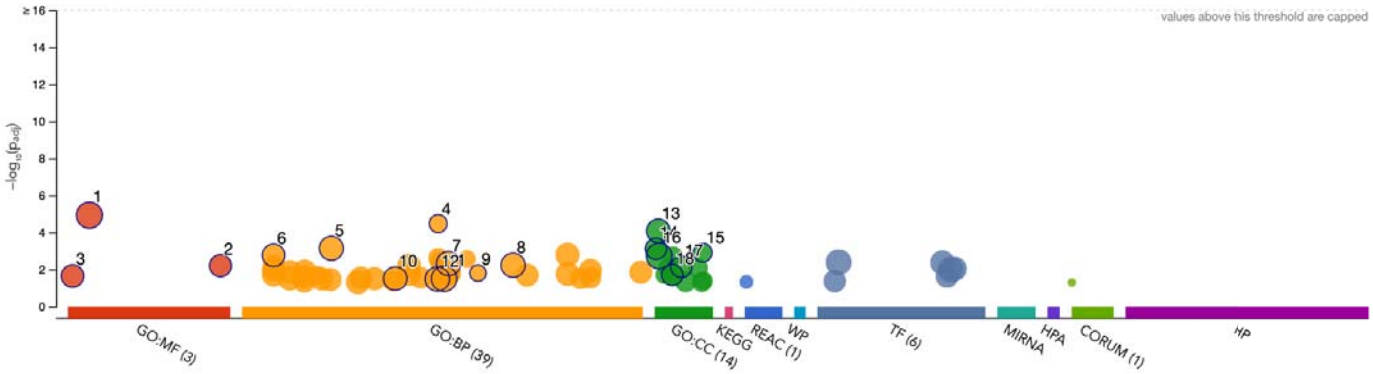

ID	Term ID	Term Name	Adjusted P-value
		GO:MF	
1	GO:0005515	protein binding	1.17E-05
2	GO:0140110	Transcription regulator activity	6.23E-03
3	GO:0003677	DNA binding	2.23E-02
		GO:BP	
4	GO:0048588	developmental cell growth	3.33E-05
5	GO:0019538	Protein metabolic process	7.18E-04
6	GO:0006357	Regulation of transcription by RNA polymerase II	4.79E-03
7	GO:0051171	Regulation of nitrogen compound metabolic processes	4.79E-03
8	GO:0080090	Regulation of primary metabolic process	5.86E-03
9	GO:0061387	Regulation of extent of cell growth	1.56E-02
10	GO:0042221	Response to chemical	3.06E-02
11	GO:0050794	Regulation of cellular process	3.13E-02
12	GO:0048518	Positive regulation of biological process	3.24E-02
		GO:CC	
13	GO:0005654	nucleoplasm	8.23E-05
14	GO:0000785	chromatin	7.56E-04
15	GO:0098984	Neuron to neuron synapse	1.22E-03
16	GO:0005737	cytoplasm	1.84E-03
17	GO:0043005	neuron projection	7.14E-03
18	GO:0031967	organelle envelope	1.96E-02

Figure 6. Functional enrichment analysis on the fine-mapped gene set identified for general cognitive function using METRO TWAS (N=266 genes). The top panel consists of a Manhattan plot that illustrates the enrichment analysis results. The x-axis represents functional terms that are grouped and color-coded by data sources, including Gene Ontology (GO): molecular function (MF; red), GO: biological process (BP; orange), GO: cellular component (CC; dark green), Kyoto Encyclopedia of Genes and Genomes (KEGG; pink), Reactome (REAC; dark blue), WikiPathways (WP; turquoise), Transfac (TF; light blue), MiRTarBase (MIRNA; emerald green), Human Protein Atlas (HPA; dark purple), CORUM protein complexes (light green), and Human Phenotype Ontology (HP; violet), in order from left to right. The y-axis shows the adjusted enriched -$\log_{10}$ p-values <0.05. Multiple testing correction was performed using g:SCS method (Set Counts and Sizes) that takes into account overlapping terms. The top panel highlights driver GO terms identified using the greedy filtering algorithm in g:Profiler. The light circles represent terms that were not significant after filtering. The circle sizes are in accordance with the corresponding term size (i.e., larger terms have larger circles). The number in parentheses following the source name in the x-axis shows how many significantly enriched terms were from this source.

medRxiv preprint doi: https://doi.org/10.1101/2024.01.03.24300768; this version posted January 5, 2024. The copyright holder for this preprint (which was not certified by peer review) is the author/funder, who has granted medRxiv a license to display the preprint in perpetuity. It is made available under a CC-BY-NC-ND 4.0 International license .

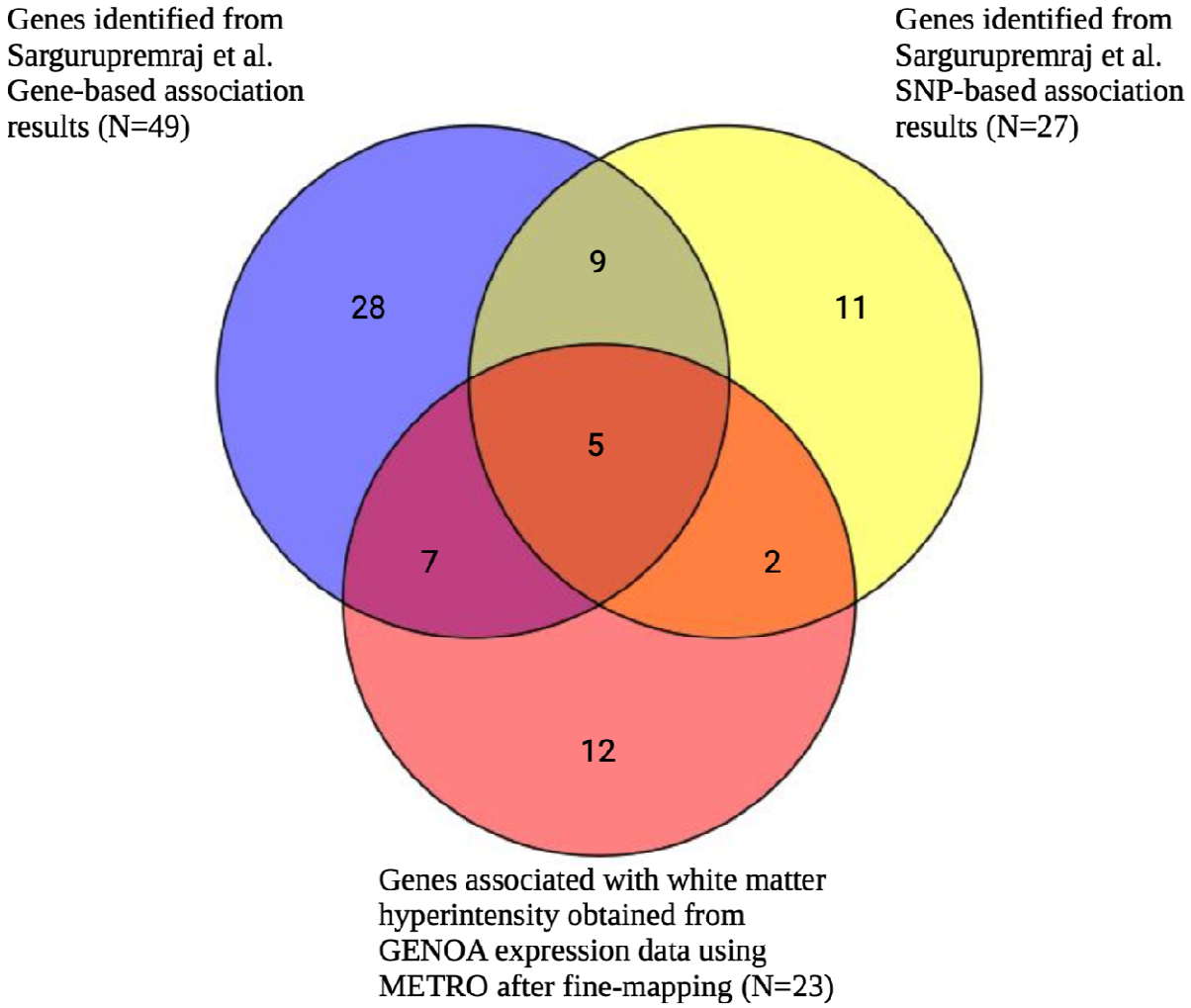

Figure 7. Venn diagram comparing number of METRO-identified genes associated with white matter hyperintensity following FOCUS fine-mapping and genes identified by Sargurupremraj et al. (2020) gene-based and SNP-based analyses.
Venn diagram comparing the number of significantly associated genes associated with white matter hyperintensity (WMH) obtained from METRO using GENOA expression data after Bonferroni correction ($P<2.90x10^{-6}$), and fine-mapping (red) and Sargurupremraj et al. (2020). Sargurupremraj et al. results included SNP-based association results that were mapped to the nearest gene ($P<5x10^{-8}$; yellow), and gene-based association results ($P<2.77x10^{-6}$; blue).

medRxiv preprint doi: https://doi.org/10.1101/2024.01.03.24300768; this version posted January 5, 2024. The copyright holder for this preprint (which was not certified by peer review) is the author/funder, who has granted medRxiv a license to display the preprint in perpetuity. It is made available under a CC-BY-NC-ND 4.0 International license .

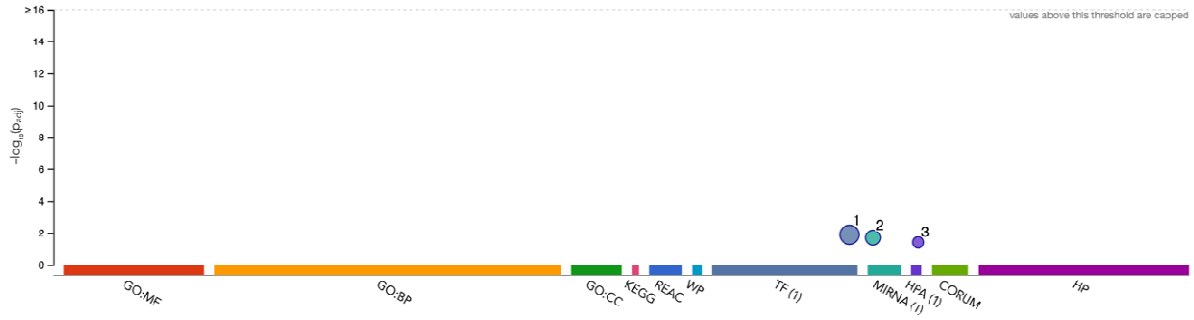

ID	Term ID	Term Name	Adjusted P-value
		TF	
1	TF:M12713	Factor: ZNF690; motif: GTCTACRCNG	1.27E-02
		MIRNA	
2	MIRNA: has-miR-212-5p	hsa-miR-212-5p	1.94E-02
		HPA	
3	HPA:0411242	Retina; inner plexiform layer [≥Medium]	3.86E-02

Figure 8. Functional enrichment analysis on the fine-mapped gene set identified for white matter hyperintensity using METRO TWAS (N=23 genes). The top panel consists of a Manhattan plot that illustrates the enrichment analysis results. The x-axis represents functional terms that are grouped and color-coded by data sources, including Gene Ontology (GO): molecular function (MF; red), GO: biological process (BP; orange), GO: cellular component (CC; dark green), Kyoto Encyclopedia of Genes and Genomes (KEGG; pink), Reactome (REAC; dark blue), WikiPathways (WP; turquoise), Transfac (TF; light blue), MiRTarBase (MIRNA; emerald green), Human Protein Atlas (HPA; dark purple), CORUM protein complexes (light green), and Human Phenotype Ontology (HP; violet), in order from left to right. The y-axis shows the adjusted enriched -$\log_{10}$ p-values < 0.05. Multiple testing correction was performed using g:SCS method (Set Counts and Sizes) that takes into account overlapping terms. The top panel highlights driver GO terms identified using the greedy filtering algorithm in g:Profiler. The light circles represent terms that were not significant after filtering. The circle sizes are in accordance with the corresponding term size (i.e., larger terms have larger circles). The number in parentheses following the source name in the x-axis shows how many significantly enriched terms were from this source.

medRxiv preprint doi: https://doi.org/10.1101/2024.01.03.24300768; this version posted January 5, 2024. The copyright holder for this preprint (which was not certified by peer review) is the author/funder, who has granted medRxiv a license to display the preprint in perpetuity. It is made available under a CC-BY-NC-ND 4.0 International license .

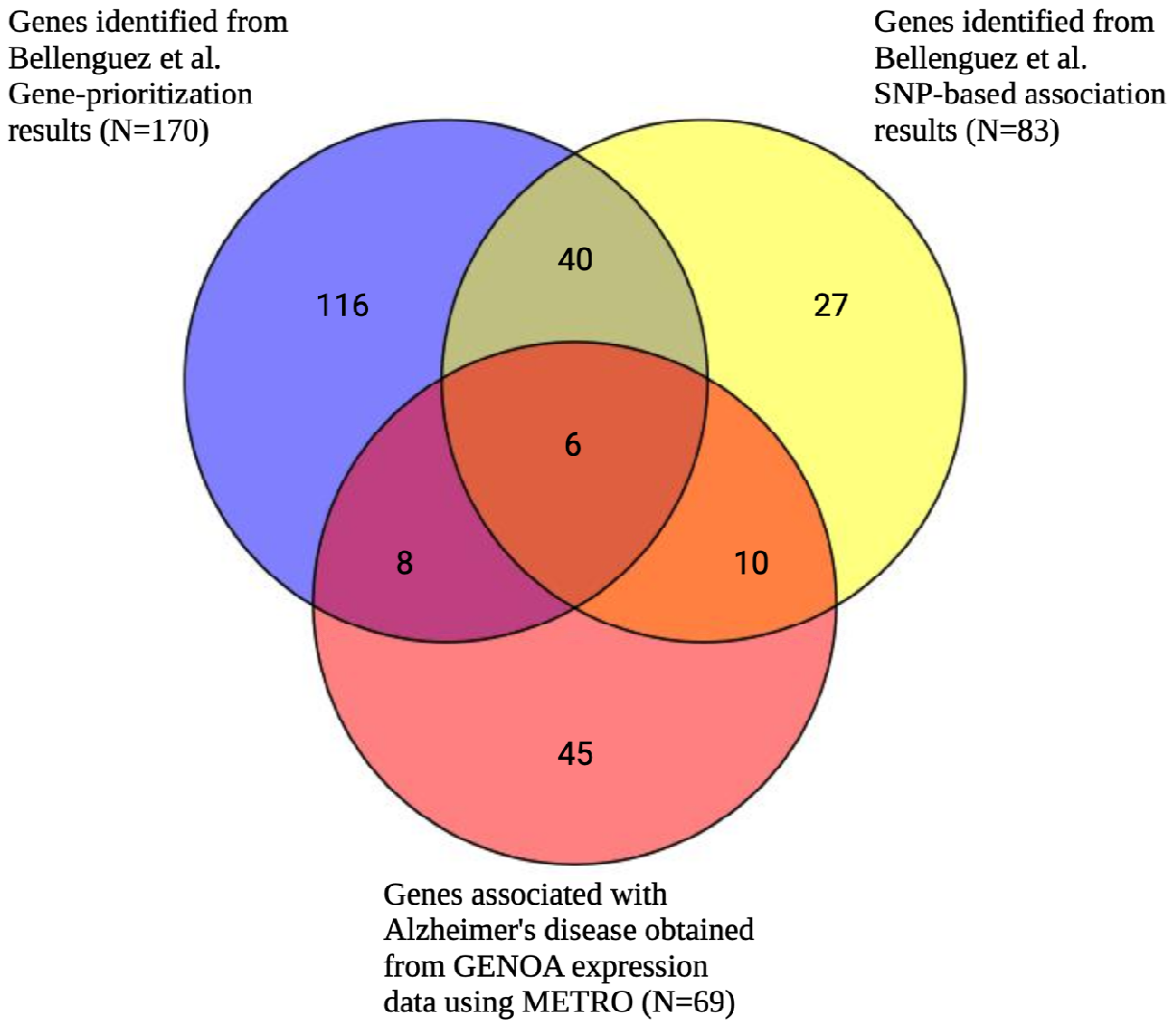

Figure 9. Venn diagram comparing number of METRO-identified genes associated with Alzheimer's disease (EA GWAS) following FOCUS fine-mapping and genes identified by Bellenguez et al. (2022) gene prioritization and SNP-based analyses.
Venn diagram comparing the number of significantly associated genes associated with Alzheimer's disease (from EA GWAS) obtained from METRO using GENOA expression data after Bonferroni correction ($P<2.90x10^{-6}$) and fine-mapping (red) and Bellenguez et al. (2022). Bellenguez et al. results included SNP-based association results that were mapped to the nearest gene ($P<5x10^{-8}$; yellow), and gene prioritization results for the genes in the novel AD risk loci (blue). In the gene prioritization analysis, Bellenguez et al. analyzed the downstream effects of new AD-associated loci on molecular phenotypes (i.e., expression, splicing, protein expression, methylation and histone acetylation) in various *cis*-quantitative trait loci (*cis*-QTL) catalogues from AD-relevant tissues, cell types and brain regions.

medRxiv preprint doi: https://doi.org/10.1101/2024.01.03.24300768; this version posted January 5, 2024. The copyright holder for this preprint (which was not certified by peer review) is the author/funder, who has granted medRxiv a license to display the preprint in perpetuity. It is made available under a CC-BY-NC-ND 4.0 International license .

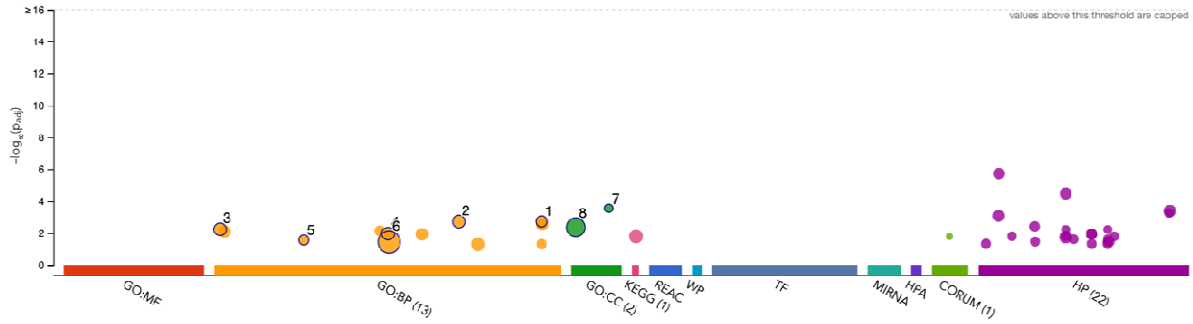

ID	Term ID	Term Name	Adjusted P-value
		GO:BP	
1	GO:1905906	regulation of amyloid fibril formation	1.87E-03
2	GO:0097242	amyloid-beta clearance	1.90E-03
3	GO:0001774	microglial cell activation	5.79E-03
4	GO:0050435	amyloid-beta metabolic process	1.07E-02
5	GO:0030450	regulation of complement activation, classical pathway	2.71E-02
6	GO:0050794	regulation of cellular process	3.60E-02
		GO: CC	
7	GO:0097418	neurofibrillary tangle	2.80E-04
8	GO:0005794	Golgi apparatus	4.39E-03

Figure 10. Functional enrichment analysis on the fine-mapped gene set identified for Alzheimer's disease (EA GWAS) using METRO TWAS (N=69 genes). The top panel consists of a Manhattan plot that illustrates the enrichment analysis results. The x-axis represents functional terms that are grouped and color-coded by data sources, including Gene Ontology (GO): molecular function (MF; red), GO: biological process (BP; orange), GO: cellular component (CC; dark green), Kyoto Encyclopedia of Genes and Genomes (KEGG; pink), Reactome (REAC; dark blue), WikiPathways (WP; turquoise), Transfac (TF; light blue), MiRTarBase (MIRNA; emerald green), Human Protein Atlas (HPA; dark purple), CORUM protein complexes (light green), and Human Phenotype Ontology (HP; violet), in order from left to right. The y-axis shows the adjusted enriched -$\log_{10}$ p-values < 0.05. Multiple testing correction was performed using g:SCS method (Set Counts and Sizes) that takes into account overlapping terms. The top panel highlights driver GO terms identified using the greedy filtering algorithm in g:Profiler. The light circles represent terms that were not significant after filtering. The circle sizes are in accordance with the corresponding term size (i.e., larger terms have larger circles). The number in parentheses following the source name in the x-axis shows how many significantly enriched terms were from this source.

medRxiv preprint doi: https://doi.org/10.1101/2024.01.03.24300768; this version posted January 5, 2024. The copyright holder for this preprint (which was not certified by peer review) is the author/funder, who has granted medRxiv a license to display the preprint in perpetuity. It is made available under a CC-BY-NC-ND 4.0 International license .

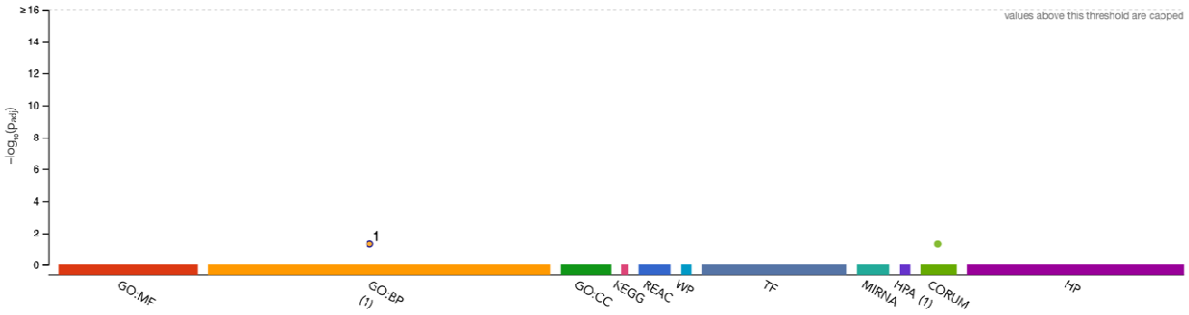

ID	Term ID	Term Name	Adjusted P-value
1	GO:0046814	Coreceptor-mediated virion attachment to host	4.96E-02

Figure 11. Functional enrichment analysis fine-mapped gene set identified for Alzheimer's disease (AA GWAS) using METRO TWAS (N=2 genes). The top panel consists of a Manhattan plot that illustrates the enrichment analysis results. The x-axis represents functional terms that are grouped and color-coded by data sources, including Gene Ontology (GO): molecular function (MF; red), GO: biological process (BP; orange), GO: cellular component (CC; dark green), Kyoto Encyclopedia of Genes and Genomes (KEGG; pink), Reactome (REAC; dark blue), WikiPathways (WP; turquoise), Transfac (TF; light blue), MiRTarBase (MIRNA; emerald green), Human Protein Atlas (HPA; dark purple), CORUM protein complexes (light green), and Human Phenotype Ontology (HP; violet), in order from left to right. The y-axis shows the adjusted enriched -$\log_{10}$ p-values < 0.05. Multiple testing correction was performed using g:SCS method (Set Counts and Sizes) that takes into account overlapping terms. The top panel highlights driver GO terms identified using the greedy filtering algorithm in g:Profiler. The light circles represent terms that were not significant after filtering. The circle sizes are in accordance with the corresponding term size (i.e., larger terms have larger circles). The number in parentheses following the source name in the x-axis shows how many significantly enriched terms were from this source.

medRxiv preprint doi: https://doi.org/10.1101/2024.01.03.24300768; this version posted January 5, 2024. The copyright holder for this preprint (which was not certified by peer review) is the author/funder, who has granted medRxiv a license to display the preprint in perpetuity. It is made available under a CC-BY-NC-ND 4.0 International license .

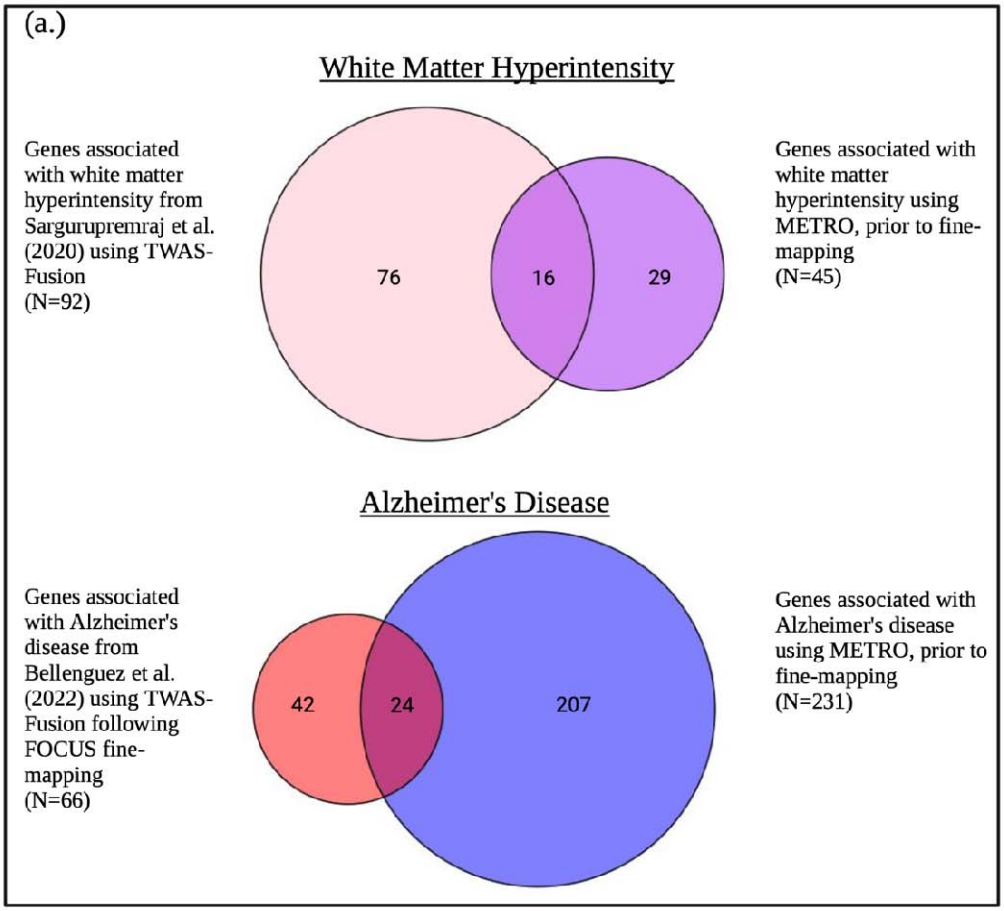

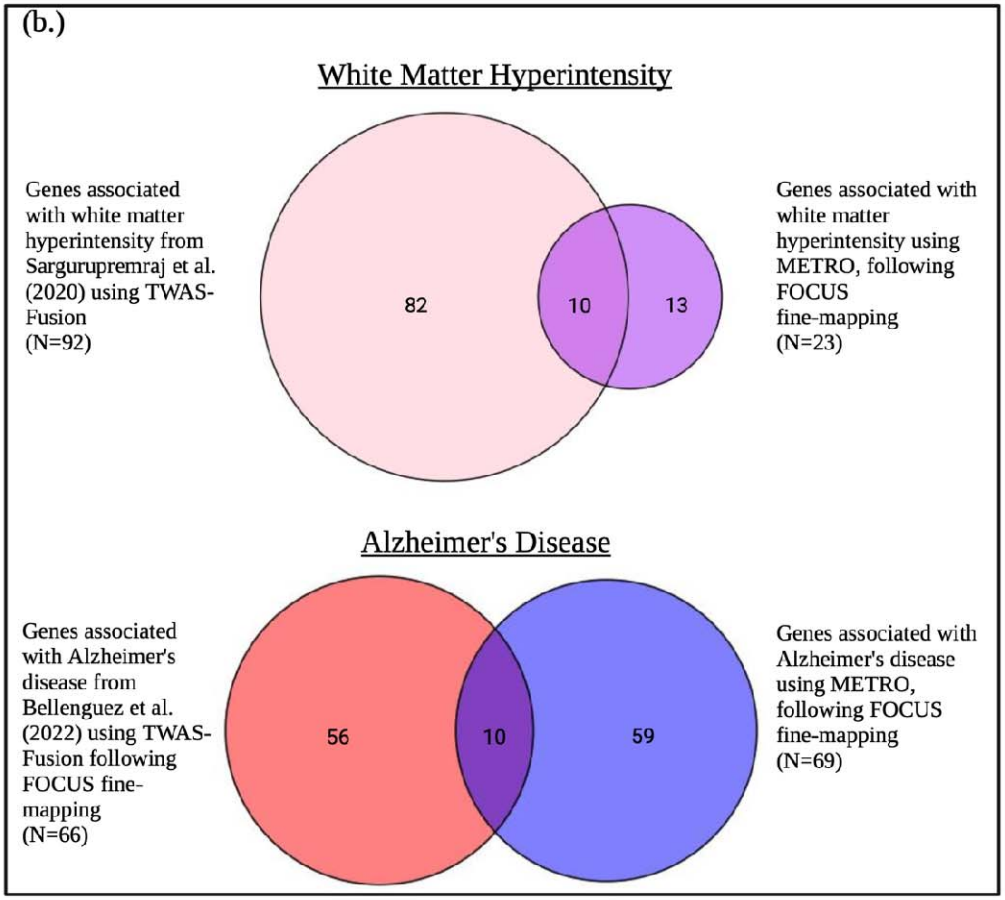

863

medRxiv preprint doi: https://doi.org/10.1101/2024.01.03.24300768; this version posted January 5, 2024. The copyright holder for this preprint (which was not certified by peer review) is the author/funder, who has granted medRxiv a license to display the preprint in perpetuity. It is made available under a CC-BY-NC-ND 4.0 International license .

Figure 12. Venn diagram comparing METRO TWAS results prior to and following FOCUS fine-mapping with TWAS results from Sargurupremraj et al. (2020) and Bellenguez et al. (2022).

Venn diagram comparing METRO TWAS results (a) prior to and (b) following FOCUS fine-mapping with TWAS results using Fusion for white matter hyperintensity from Sargurupremraj et al. (2020) without fine-mapping and Alzheimer's disease from Bellenguez et al. (2022) (EA GWAS) with FOCUS fine-mapping.

medRxiv preprint doi: https://doi.org/10.1101/2024.01.03.24300768; this version posted January 5, 2024. The copyright holder for this preprint (which was not certified by peer review) is the author/funder, who has granted medRxiv a license to display the preprint in perpetuity. It is made available under a CC-BY-NC-ND 4.0 International license .

References

1. 2023 Alzheimer's disease facts and figures. Alzheimer's & Dementia. 2023 Apr;19(4):1598–695.

2. De Reuck J, Maurage CA, Deramecourt V, Pasquier F, Cordonnier C, Leys D, et al. Aging and cerebrovascular lesions in pure and in mixed neurodegenerative and vascular dementia brains: a neuropathological study. Folia Neuropathol. 2018;56(2):81–7.

3. Hof PR, Glannakopoulos P, Bouras C. The neuropathological changes associated with normal brain aging. Histol Histopathol. 1996 Oct;11(4):1075–88.

4. Perl DP. Neuropathology of Alzheimer's Disease. Mt Sinai J Med. 2010;77(1):32–42.

5. Cohuet G, Struijker-Boudier H. Mechanisms of target organ damage caused by hypertension: Therapeutic potential. Pharmacology & Therapeutics. 2006 Jul 1;111(1):81–98.

6. Weller J, Budson A. Current understanding of Alzheimer's disease diagnosis and treatment. F1000Res. 2018 Jul 31;7:F1000 Faculty Rev-1161.

7. Hubbard BM, Fenton GW, Anderson JM. A quantitative histological study of early clinical and preclinical Alzheimer's disease. Neuropathol Appl Neurobiol. 1990 Apr;16(2):111–21.

8. Sperling RA, Aisen PS, Beckett LA, Bennett DA, Craft S, Fagan AM, et al. Toward defining the preclinical stages of Alzheimer's disease: recommendations from the National Institute on Aging-Alzheimer's Association workgroups on diagnostic guidelines for Alzheimer's disease. Alzheimers Dement. 2011 May;7(3):280–92.

9. Mayeda ER, Glymour MM, Quesenberry CP, Whitmer RA. Inequalities in dementia incidence between six racial and ethnic groups over 14 years. Alzheimers Dement. 2016 Mar;12(3):216–24.

10. Barnes LL, Bennett DA. Alzheimer's disease in African Americans: risk factors and challenges for the future. Health Aff (Millwood). 2014 Apr;33(4):580–6.

11. Brewster P, Barnes L, Haan M, Johnson JK, Manly JJ, Nápoles AM, et al. Progress and future challenges in aging and diversity research in the United States. Alzheimers Dement. 2019 Jul;15(7):995–1003.

12. Rajan KB, Weuve J, Barnes LL, Wilson RS, Evans DA. Prevalence and incidence of clinically diagnosed Alzheimer's disease dementia from 1994 to 2012 in a population study. Alzheimers Dement. 2019 Jan;15(1):1–7.

13. Cacabelos R, Torrellas C. Epigenetics of Aging and Alzheimer's Disease: Implications for Pharmacogenomics and Drug Response. International Journal of Molecular Sciences. 2015 Dec;16(12):30483–543.

medRxiv preprint doi: https://doi.org/10.1101/2024.01.03.24300768; this version posted January 5, 2024. The copyright holder for this preprint (which was not certified by peer review) is the author/funder, who has granted medRxiv a license to display the preprint in perpetuity. It is made available under a CC-BY-NC-ND 4.0 International license .

14. Tam V, Patel N, Turcotte M, Bossé Y, Paré G, Meyre D. Benefits and limitations of genome-wide association studies. Nat Rev Genet. 2019 Aug;20(8):467–84.

15. Lappalainen T, Sammeth M, Friedländer MR, ‘t Hoen PA, Monlong J, Rivas MA, et al. Transcriptome and genome sequencing uncovers functional variation in humans. Nature. 2013 Sep 26;501(7468):506–11.

16. Mogil LS, Andaleon A, Badalamenti A, Dickinson SP, Guo X, Rotter JI, et al. Genetic architecture of gene expression traits across diverse populations. PLOS Genetics. 2018 Aug 10;14(8):e1007586.

17. Wojcik G, Graff M, Nishimura K, Tao R, Haessler J, Gignoux C, et al. Genetic analyses of diverse populations improves discovery for complex traits. Nature. 2019;570(7762):514–8.

18. Shang L, Smith JA, Zhao W, Kho M, Turner ST, Mosley TH, et al. Genetic Architecture of Gene Expression in European and African Americans: An eQTL Mapping Study in GENOA. Am J Hum Genet. 2020 Apr 2;106(4):496–512.

19. Nica AC, Dermitzakis ET. Expression quantitative trait loci: present and future. Philos Trans R Soc Lond B Biol Sci. 2013 Jun 19;368(1620):20120362.

20. Li Z, Zhao W, Shang L, Mosley TH, Kardia SLR, Smith JA, et al. METRO: Multi-ancestry transcriptome-wide association studies for powerful gene-trait association detection. The American Journal of Human Genetics. 2022 May 5;109(5):783–801.

21. Davies G, Lam M, Harris SE, Trampush JW, Luciano M, Hill WD, et al. Study of 300,486 individuals identifies 148 independent genetic loci influencing general cognitive function. Nat Commun. 2018 May 29;9(1):2098.

22. Sargurupremraj M, Suzuki H, Jian X, Sarnowski C, Evans TE, Bis JC, et al. Cerebral small vessel disease genomics and its implications across the lifespan. Nature Communications. 2020 Dec 8;11(1):6285.

23. Bellenguez C, Küçükali F, Jansen IE, Kleineidam L, Moreno-Grau S, Amin N, et al. New insights into the genetic etiology of Alzheimer’s disease and related dementias. Nat Genet. 2022 Apr 4;1–25.

24. Kunkle BW, Schmidt M, Klein HU, Naj AC, Hamilton-Nelson KL, Larson EB, et al. Novel Alzheimer Disease Risk Loci and Pathways in African American Individuals Using the African Genome Resources Panel: A Meta-analysis. JAMA Neurol. 2021 Jan 1;78(1):102–13.

25. Daniels PR, Kardia SLR, Hanis CL, Brown CA, Hutchinson R, Boerwinkle E, et al. Familial aggregation of hypertension treatment and control in the Genetic Epidemiology Network of Arteriopathy (GENOA) study. Am J Med. 2004 May 15;116(10):676–81.

26. Delaneau O, Zagury JF, Marchini J. Improved whole-chromosome phasing for disease and population genetic studies. Nat Methods. 2013 Jan;10(1):5–6.

medRxiv preprint doi: https://doi.org/10.1101/2024.01.03.24300768; this version posted January 5, 2024. The copyright holder for this preprint (which was not certified by peer review) is the author/funder, who has granted medRxiv a license to display the preprint in perpetuity. It is made available under a CC-BY-NC-ND 4.0 International license .

27. Howie BN, Donnelly P, Marchini J. A Flexible and Accurate Genotype Imputation Method for the Next Generation of Genome-Wide Association Studies. PLOS Genetics. 2009 Jun 19;5(6):e1000529.

28. Gogarten SM, Sofer T, Chen H, Yu C, Brody JA, Thornton TA, et al. Genetic association testing using the GENESIS R/Bioconductor package. Bioinformatics. 2019;35(24):5346–8.

29. Lockstone HE. Exon array data analysis using Affymetrix power tools and R statistical software. Briefings in Bioinformatics. 2011 Nov 1;12(6):634–44.

30. Irizarry RA, Bolstad BM, Collin F, Cope LM, Hobbs B, Speed TP. Summaries of Affymetrix GeneChip probe level data. Nucleic Acids Research. 2003 Feb 15;31(4):e15.

31. Dai M, Wang P, Boyd AD, Kostov G, Athey B, Jones EG, et al. Evolving gene/transcript definitions significantly alter the interpretation of GeneChip data. Nucleic Acids Research. 2005 Nov 1;33(20):e175.

32. Johnson WE, Li C, Rabinovic A. Adjusting batch effects in microarray expression data using empirical Bayes methods. Biostatistics. 2007 Jan 1;8(1):118–27.

33. Harrow J, Frankish A, Gonzalez JM, Tapanari E, Diekhans M, Kokocinski F, et al. GENCODE: the reference human genome annotation for The ENCODE Project. Genome research. 2012;22(9):1760–74.

34. Gusev A, Ko A, Shi H, Bhatia G, Chung W, Penninx BWJH, et al. Integrative approaches for large-scale transcriptome-wide association studies. Nat Genet. 2016 Mar;48(3):245–52.

35. Barbeira AN, Bonazzola R, Gamazon ER, Liang Y, Park Y, Kim-Hellmuth S, et al. Exploiting the GTEx resources to decipher the mechanisms at GWAS loci. Genome Biology. 2021 Jan 26;22(1):49.

36. THE GTEX CONSORTIUM. The GTEx Consortium atlas of genetic regulatory effects across human tissues. Science. 2020 Sep 11;369(6509):1318–30.

37. Mancuso N, Freund MK, Johnson R, Shi H, Kichaev G, Gusev A, et al. Probabilistic fine-mapping of transcriptome-wide association studies. Nature genetics. 2019;51(4):675–82.

38. Turner SD. qqman: an R package for visualizing GWAS results using Q-Q and manhattan plots [Internet]. bioRxiv; 2014 [cited 2023 Jun 6]. p. 005165. Available from: https://www.biorxiv.org/content/10.1101/005165v1

39. Berisa T, Pickrell JK. Approximately independent linkage disequilibrium blocks in human populations. Bioinformatics. 2016;32(2):283.

40. Chen H, Boutros PC. VennDiagram: a package for the generation of highly-customizable Venn and Euler diagrams in R. BMC Bioinformatics. 2011 Jan 26;12(1):35.

medRxiv preprint doi: https://doi.org/10.1101/2024.01.03.24300768; this version posted January 5, 2024. The copyright holder for this preprint (which was not certified by peer review) is the author/funder, who has granted medRxiv a license to display the preprint in perpetuity. It is made available under a CC-BY-NC-ND 4.0 International license .

41. de Leeuw CA, Stringer S, Dekkers IA, Heskes T, Posthuma D. Conditional and interaction gene-set analysis reveals novel functional pathways for blood pressure. Nat Commun. 2018 Sep 14;9(1):3768.

42. Mancarcı BO. Gene Synonym [Internet]. 2022 [cited 2023 Jul 6]. Available from: https://github.com/oganm/geneSynonym

43. Raudvere U, Kolberg L, Kuzmin I, Arak T, Adler P, Peterson H, et al. g:Profiler: a web server for functional enrichment analysis and conversions of gene lists (2019 update). Nucleic Acids Research. 2019 Jul 2;47(W1):W191–8.

44. Chagnot A, Barnes SR, Montagne A. Magnetic Resonance Imaging of Blood–Brain Barrier permeability in Dementia. Neuroscience. 2021 Oct 15;474:14–29.

45. Kalaria RN, Sepulveda-Falla D. Cerebral Small Vessel Disease in Sporadic and Familial Alzheimer Disease. The American Journal of Pathology. 2021 Nov 1;191(11):1888–905.

46. Zhang C, Qin F, Li X, Du X, Li T. Identification of novel proteins for lacunar stroke by integrating genome-wide association data and human brain proteomes. BMC Medicine. 2022 Jun 23;20(1):211.

47. Bai B, Vanderwall D, Li Y, Wang X, Poudel S, Wang H, et al. Proteomic landscape of Alzheimer's Disease: novel insights into pathogenesis and biomarker discovery. Mol Neurodegener. 2021 Aug 12;16:55.

48. Wingo AP, Liu Y, Gerasimov ES, Gockley J, Logsdon BA, Duong DM, et al. Integrating human brain proteomes with genome-wide association data implicates new proteins in Alzheimer's disease pathogenesis. Nat Genet. 2021 Feb;53(2):143–6.

49. Ou YN, Yang YX, Deng YT, Zhang C, Hu H, Wu BS, et al. Identification of novel drug targets for Alzheimer's disease by integrating genetics and proteomes from brain and blood. Mol Psychiatry. 2021 Oct;26(10):6065–73.

50. Cullell N, Gallego-Fábrega C, Cárcel-Márquez J, Muiño E, Llucià-Carol L, Lledós M, et al. ICA1L Is Associated with Small Vessel Disease: A Proteome-Wide Association Study in Small Vessel Stroke and Intracerebral Haemorrhage. Int J Mol Sci. 2022 Mar 15;23(6):3161.

51. Liu DZ, Sharp FR. Excitatory and Mitogenic Signaling in Cell Death, Blood–brain Barrier Breakdown, and BBB Repair after Intracerebral Hemorrhage. Transl Stroke Res. 2012 Jul 1;3(1):62–9.

52. Lai TW, Zhang S, Wang YT. Excitotoxicity and stroke: Identifying novel targets for neuroprotection. Progress in Neurobiology. 2014 Apr 1;115:157–88.

53. Ge YJ, Ou YN, Deng YT, Wu BS, Yang L, Zhang YR, et al. Prioritization of Drug Targets for Neurodegenerative Diseases by Integrating Genetic and Proteomic Data From Brain and Blood. Biological Psychiatry. 2023 May 1;93(9):770–9.

medRxiv preprint doi: https://doi.org/10.1101/2024.01.03.24300768; this version posted January 5, 2024. The copyright holder for this preprint (which was not certified by peer review) is the author/funder, who has granted medRxiv a license to display the preprint in perpetuity. It is made available under a CC-BY-NC-ND 4.0 International license .

54. Kanehisa M, Furumichi M, Sato Y, Ishiguro-Watanabe M, Tanabe M. KEGG: integrating viruses and cellular organisms. Nucleic Acids Research. 2021 Jan 8;49(D1):D545–51.

55. De Bruijn MF, Speck NA. Core-binding factors in hematopoiesis and immune function. Oncogene. 2004 May 24;23(24):4238–48.

56. Maillard I, Adler SH, Pear WS. Notch and the Immune System. Immunity. 2003 Dec;19(6):781–91.

57. Radtke F, Wilson A, Mancini SJC, MacDonald HR. Notch regulation of lymphocyte development and function. Nat Immunol. 2004 Mar;5(3):247–53.

58. Rothenberg EV, Taghon T. MOLECULAR GENETICS OF T CELL DEVELOPMENT. Annu Rev Immunol. 2005 Apr 1;23(1):601–49.

59. Shapiro-Shelef M, Calame K. Regulation of plasma-cell development. Nat Rev Immunol. 2005 Mar;5(3):230–42.

60. Spits H. Development of αβ T cells in the human thymus. Nat Rev Immunol. 2002 Oct;2(10):760–72.

61. Lambert JC, Ibrahim-Verbaas CA, Harold D, Naj AC, Sims R, Bellenguez C, et al. Meta-analysis of 74,046 individuals identifies 11 new susceptibility loci for Alzheimer's disease. Nat Genet. 2013 Dec;45(12):1452–8.

62. Hollingworth P, Harold D, Sims R, Gerrish A, Lambert JC, Carrasquillo MM, et al. Common variants in ABCA7, MS4A6A/MS4A4E, EPHA1, CD33 and CD2AP are associated with Alzheimer's disease. Nat Genet. 2011 May;43(5):429–35.

63. Reitz C, Mayeux R. Genetics of Alzheimer's Disease in Caribbean Hispanic and African American Populations. Biological Psychiatry. 2014 Apr;75(7):534–41.

64. Reitz C, Jun G, Naj A, Rajbhandary R. Variants in the ATP-Binding Cassette Transporter (ABCA7), Apolipoprotein E □4,and the Risk of Late-Onset Alzheimer Disease in African Americans. JAMA. 2013 Apr 10;309(14):1483–92.

65. De Roeck A, Van Broeckhoven C, Sleegers K. The role of ABCA7 in Alzheimer's disease: evidence from genomics, transcriptomics and methylomics. Acta Neuropathol. 2019 Aug 1;138(2):201–20.

66. Guardiola M, Muntané G, Martínez I, Martorell L, Girona J, Ibarretxe D, et al. Metabolic Overlap between Alzheimer's Disease and Metabolic Syndrome Identifies the PVRL2 Gene as a New Modulator of Diabetic Dyslipidemia. Int J Mol Sci. 2023 Apr 18;24(8):7415.

67. Liang X, Liu C, Liu K, Cong L, Wang Y, Liu R, et al. Association and interaction of TOMM40 and PVRL2 with plasma amyloid-β and Alzheimer's disease among Chinese older adults: a population-based study. Neurobiol Aging. 2022 May;113:143–51.

medRxiv preprint doi: https://doi.org/10.1101/2024.01.03.24300768; this version posted January 5, 2024. The copyright holder for this preprint (which was not certified by peer review) is the author/funder, who has granted medRxiv a license to display the preprint in perpetuity. It is made available under a CC-BY-NC-ND 4.0 International license .

68. Chatterjee P, Roy D, Bhattacharyya M, Bandyopadhyay S. Biological networks in Parkinson's disease: an insight into the epigenetic mechanisms associated with this disease. BMC Genomics. 2017 Sep 12;18(1):721.

69. Gialluisi A, Reccia MG, Modugno N, Nutile T, Lombardi A, Di Giovannantonio LG, et al. Identification of sixteen novel candidate genes for late onset Parkinson's disease. Mol Neurodegener. 2021 Jun 21;16(1):35.

70. Salem M, Ammitzboell M, Nys K, Seidelin JB, Nielsen OH. ATG16L1: A multifunctional susceptibility factor in Crohn disease. Autophagy. 2015 Apr 23;11(4):585–94.

71. Hansson O, Kumar A, Janelidze S, Stomrud E, Insel PS, Blennow K, et al. The genetic regulation of protein expression in cerebrospinal fluid. EMBO Mol Med. 2023 Jan 11;15(1):e16359.

72. Cali E, Dominik N, Manole A, Houlden H. Riboflavin Transporter Deficiency. In: Adam MP, Mirzaa GM, Pagon RA, Wallace SE, Bean LJ, Gripp KW, et al., editors. GeneReviews® [Internet]. Seattle (WA): University of Washington, Seattle; 1993 [cited 2023 Jul 31]. Available from: http://www.ncbi.nlm.nih.gov/books/NBK299312/

73. Novikova G, Kapoor M, Tcw J, Abud EM, Efthymiou AG, Chen SX, et al. Integration of Alzheimer's disease genetics and myeloid genomics identifies disease risk regulatory elements and genes. Nat Commun. 2021 Mar 12;12(1):1610.

74. Allan CM, Walker D, Segrest JP, Taylor JM. Identification and characterization of a new human gene (APOC4) in the apolipoprotein E, C-I, and C-II gene locus. Genomics. 1995 Jul 20;28(2):291–300.

75. Wang P, Luo M, Zhou W, Jin X, Xu Z, Yan S, et al. Global Characterization of Peripheral B Cells in Parkinson's Disease by Single-Cell RNA and BCR Sequencing. Front Immunol. 2022;13:814239.

76. Lp Y, Mj S. The cryptic HLA-DQA2 ("DX alpha") gene is expressed in human B cell lines. Journal of immunology (Baltimore, Md□: 1950) [Internet]. 1991 Dec 15 [cited 2023 Aug 4];147(12). Available from: https://pubmed.ncbi.nlm.nih.gov/1753107/

77. Li GJ, Yang QH, Yang GK, Yang G, Hou Y, Hou LJ, et al. MiR-125b and SATB1-AS1 might be shear stress-mediated therapeutic targets. Gene. 2023 Mar 20;857:147181.

78. Naguib A, Sandmann T, Yi F, Watts RJ, Lewcock JW, Dowdle WE. SUPT4H1 Depletion Leads to a Global Reduction in RNA. Cell Rep. 2019 Jan 2;26(1):45-53.e4.

79. Greaves CV, Rohrer JD. An update on genetic frontotemporal dementia. J Neurol. 2019 Aug;266(8):2075–86.

80. Ballasch I, García-García E, Vila C, Pérez-González A, Sancho-Balsells A, Fernández J, et al. Ikzf1 as a novel regulator of microglial homeostasis in inflammation and neurodegeneration. Brain Behav Immun. 2023 Mar;109:144–61.

medRxiv preprint doi: https://doi.org/10.1101/2024.01.03.24300768; this version posted January 5, 2024. The copyright holder for this preprint (which was not certified by peer review) is the author/funder, who has granted medRxiv a license to display the preprint in perpetuity. It is made available under a CC-BY-NC-ND 4.0 International license .

81. Schutte B, Henfling M, Ramaekers FCS. DEDD association with cytokeratin filaments correlates with sensitivity to apoptosis. Apoptosis. 2006 Sep;11(9):1561–72.

82. Dahal A, Hinton SD. Antagonistic roles for STYX pseudophosphatases in neurite outgrowth. Biochem Soc Trans. 2017 Apr 15;45(2):381–7.

83. Burgaletto C, Munafò A, Di Benedetto G, De Francisci C, Caraci F, Di Mauro R, et al. The immune system on the TRAIL of Alzheimer's disease. Journal of Neuroinflammation. 2020 Oct 13;17(1):298.

84. Traylor M, Persyn E, Tomppo L, Klasson S, Abedi V, Bakker MK, et al. Genetic basis of lacunar stroke: a pooled analysis of individual patient data and genome-wide association studies. Lancet Neurol. 2021 May;20(5):351–61.

85. Chen K, Zhu L, Guo L, Pan YB, Feng DF. Maf1 regulates dendritic morphogenesis and influences learning and memory. Cell Death Dis. 2020 Jul 30;11(7):606.

86. Kumar AA, Yeo N, Whittaker M, Attra P, Barrick TR, Bridges LR, et al. Vascular Collagen Type-IV in Hypertension and Cerebral Small Vessel Disease. Stroke. 2022 Dec;53(12):3696–705.

87. Miners S, van Helmond Z, Barker R, Passmore PA, Johnston JA, Todd S, et al. Genetic variation in MME in relation to neprilysin protein and enzyme activity, Aβ levels, and Alzheimer's disease risk. Int J Mol Epidemiol Genet. 2012;3(1):30–8.

88. Chen G, Li L, Tao H. Bioinformatics Identification of Ferroptosis-Related Biomarkers and Therapeutic Compounds in Ischemic Stroke. Front Neurol. 2021;12:745240.

89. Pan Y, Fu Y, Baird PN, Guymer RH, Das T, Iwata T. Exploring the contribution of ARMS2 and HTRA1 genetic risk factors in age-related macular degeneration. Prog Retin Eye Res. 2022 Dec 27;101159.

90. Thee EF, Colijn JM, Cougnard-Grégoire A, Meester-Smoor MA, Verzijden T, Hoyng CB, et al. The Phenotypic Course of Age-Related Macular Degeneration for ARMS2/HTRA1: The EYE-RISK Consortium. Ophthalmology. 2022 Jul;129(7):752–64.

91. Gatta LB, Vitali M, Zanola A, Venturelli E, Fenoglio C, Galimberti D, et al. Polymorphisms in the LOC387715/ARMS2 putative gene and the risk for Alzheimer's disease. Dement Geriatr Cogn Disord. 2008;26(2):169–74.

92. Wang P, Qin W, Wang P, Huang Y, Liu Y, Zhang R, et al. Genomic Variants in NEURL, GJA1 and CUX2 Significantly Increase Genetic Susceptibility to Atrial Fibrillation. Sci Rep. 2018 Feb 19;8(1):3297.

93. Li RG, Xu YJ, Ye WG, Li YJ, Chen H, Qiu XB, et al. Connexin45 (GJC1) loss-of-function mutation contributes to familial atrial fibrillation and conduction disease. Heart Rhythm. 2021 May;18(5):684–93.

medRxiv preprint doi: https://doi.org/10.1101/2024.01.03.24300768; this version posted January 5, 2024. The copyright holder for this preprint (which was not certified by peer review) is the author/funder, who has granted medRxiv a license to display the preprint in perpetuity. It is made available under a CC-BY-NC-ND 4.0 International license .

94. Zhu C, Xiao F, Lin W. EFTUD2 on innate immunity. Oncotarget. 2015 Oct 20;6(32):32313–4.

95. Abo Elwafa R, Gamaleldin M, Ghallab O. The clinical and prognostic significance of FIS1, SPI1, PDCD7 and Ang2 expression levels in acute myeloid leukemia. Cancer Genet. 2019 Apr;233–234:84–95.

96. Vadhvani M, Schwedhelm-Domeyer N, Mukherjee C, Stegmüller J. The centrosomal E3 ubiquitin ligase FBXO31-SCF regulates neuronal morphogenesis and migration. PLoS One. 2013;8(2):e57530.

97. Serpeloni F, Nätt D, Assis SG de, Wieling E, Elbert T. Experiencing community and domestic violence is associated with epigenetic changes in DNA methylation of BDNF and CLPX in adolescents. Psychophysiology. 2020;57(1):e13382.

98. ZSCAN29 zinc finger and SCAN domain containing 29 [Homo sapiens (human)] - Gene - NCBI [Internet]. [cited 2023 Aug 1]. Available from: https://www.ncbi.nlm.nih.gov/gene/146050#summary

99. Baker TA, Sauer RT. ClpXP, an ATP-powered unfolding and protein-degradation machine. Biochimica et Biophysica Acta (BBA) - Molecular Cell Research. 2012 Jan 1;1823(1):15–28.

100. Thomas T, Perdue MV, Khalaf S, Landi N, Hoeft F, Pugh K, et al. Neuroimaging genetic associations between SEMA6D, brain structure, and reading skills. J Clin Exp Neuropsychol. 2021 Apr;43(3):276–89.

101. Perdue MV, Mascheretti S, Kornilov SA, Jasińska KK, Ryherd K, Einar Mencl W, et al. Common variation within the SETBP1 gene is associated with reading-related skills and patterns of functional neural activation. Neuropsychologia. 2019 Jul;130:44–51.

102. Ziegler GC, Ehlis AC, Weber H, Vitale MR, Zöller JEM, Ku HP, et al. A Common CDH13 Variant Is Associated with Low Agreeableness and Neural Responses to Working Memory Tasks in ADHD. Genes. 2021 Sep;12(9):1356.

103. Trubetskoy V, Pardiñas AF, Qi T, Panagiotaropoulou G, Awasthi S, Bigdeli TB, et al. Mapping genomic loci implicates genes and synaptic biology in schizophrenia. Nature. 2022 Apr;604(7906):502–8.

104. Beeri MS, Lin HM, Sano M, Ravona-Springer R, Liu X, Bendlin BB, et al. Association of the Haptoglobin Gene Polymorphism With Cognitive Function and Decline in Elderly African American Adults With Type 2 Diabetes: Findings From the Action to Control Cardiovascular Risk in Diabetes-Memory in Diabetes (ACCORD-MIND) Study. JAMA Netw Open. 2018 Nov 2;1(7):e184458.

105. Kikuchi M, Yamada K, Toyota T, Yoshikawa T. C18orf1 located on chromosome 18p11.2 may confer susceptibility to schizophrenia. J Med Dent Sci. 2003 Sep;50(3):225–9.

medRxiv preprint doi: https://doi.org/10.1101/2024.01.03.24300768; this version posted January 5, 2024. The copyright holder for this preprint (which was not certified by peer review) is the author/funder, who has granted medRxiv a license to display the preprint in perpetuity. It is made available under a CC-BY-NC-ND 4.0 International license .

106. Zhang Z, Shang J, Dai Z, Yao Y, Shi Y, Zhong D, et al. Transmembrane Protein 170B is a Prognostic Biomarker and Associated With Immune Infiltrates in Pancreatic Adenocarcinoma. Front Genet. 2022;13:848391.

107. Ge Y, Grossman RI, Babb JS, Rabin ML, Mannon LJ, Kolson DL. Age-Related Total Gray Matter and White Matter Changes in Normal Adult Brain. Part I: Volumetric MR Imaging Analysis. American Journal of Neuroradiology. 2002 Sep 1;23(8):1327–33.

108. Davies G, Armstrong N, Bis JC, Bressler J, Chouraki V, Giddaluru S, et al. Genetic contributions to variation in general cognitive function: a meta-analysis of genome-wide association studies in the CHARGE consortium (N=53 949). Mol Psychiatry. 2015 Feb;20(2):183–92.

109. Dumitrescu L, Mahoney ER, Mukherjee S, Lee ML, Bush WS, Engelman CD, et al. Genetic variants and functional pathways associated with resilience to Alzheimer's disease. Brain. 2020 Aug 25;143(8):2561–75.

110. Fridman AL, Tainsky MA. Critical pathways in cellular senescence and immortalization revealed by gene expression profiling. Oncogene. 2008 Oct;27(46):5975–87.

111. Wainberg M, Sinnott-Armstrong N, Mancuso N, Barbeira AN, Knowles DA, Golan D, et al. Opportunities and challenges for transcriptome-wide association studies. Nat Genet. 2019 Apr;51(4):592–9.

112. Wu C, Pan W. A powerful fine-mapping method for transcriptome-wide association studies. Hum Genet. 2020 Feb;139(2):199–213.